MODELING OF RF ENERGY HARVESTING AND ENERGY CONSUMPTION SYSTEM FOR LOW POWER WIRELESS SENSOR NETWORKS

A Thesis

by

Osama Amjad

Submitted to the
Graduate School of Sciences and Engineering
In Partial Fulfillment of the Requirements for
the Degree of

Master of Science

in the
Department of Electrical and Electronics Engineering

Özyeğin University
January 2017

MODELING OF RF ENERGY HARVESTING AND ENERGY CONSUMPTION SYSTEM FOR LOW POWER WIRELESS SENSOR NETWORKS

Approved by:

Asst. Prof. Ali Özer Ercan, Advisor
Department of Electrical and Electronics Engineering
Özyeğin University

Assoc. Prof. Onur Kaya
Department of Electrical and Electronics Engineering
Işık University

Asst. Prof. Ahmet Tekin
Department of Electrical and Electronics Engineering
Özyeğin University

Date Approved: 05 January 2017

To my parents and family for there support and encouragement.....

ABSTRACT

Recently, with the advancement of technology, there has been a rapid growth of low power wireless devices, such as wireless sensor networks (WSNs) and Internet of Things (IoT). Therefore, the energy requirement for perpetual operation of these devices has also been increased. However, in comparison the evolution of battery technologies is not yet capable to meet the energy demand, thus there exists a huge gap between the energy demand of the wireless devices and the energy density resulting from the development in battery technology. Therefore, the major challenge is to find an alternative and promising source of energy that enables self sustained sensor node operations.

In this regard, the concept of wireless energy harvesting from ambient green sources (e.g., solar, thermal, vibrational, RF) has gained much importance to power these devices. Among other sources, RF source is a potential candidate for energy harvesting due to continuous availability of RF signals. However, there exist critical challenges that need to be tackled, such as design and implementation of RF energy harvesting systems. The presented work demonstrates the design and analysis of RF energy harvesting from cellular base stations, operating simultaneously at 900 MHz and 1800 MHz. Moreover, the effect of real time wireless channel on total harvested energy has been investigated, which is a novel aspect of this work. In addition, application of RF energy harvesting in WSNs has been discussed that aims to report the power consumption demand of a sensor node under different states. For this purpose, OpenMote hardware (the latest generation of Berkeley motes) has been used to perform experiments and to measure the power consumption demand under different states (e.g., sensing, transmission and reception).

ÖZETÇE

Yakın geçmişteki teknolojik ilerlemelerin sonucu olarak, telsiz algılayıcı ağlar (*İng. Wireless Sensor Networks, WSNs*) ve Nesnelerin İnterneti (*İng. Internet of Things, IoT*) gibi az enerji kullanan telsiz uygulamalarında büyük bir artış görülmüştür. Bu cihazların devamlı çalışabilmesi için enerji gereksinimleri de artmıştır. Öte yandan günümüz pil teknolojilerinin bu gereksinimi karşılayabilmesi mümkün değildir, telsiz cihazların enerji ihtiyaçları ve pil teknolojisinin gelişiminden ortaya çıkan pil enerji yoğunluğu arasında büyük bir boşluk bulunmaktadır. Dolayısı ile algılayıcı ağların devamlı çalışabilmesini sağlayacak alternatif bir enerji kaynağı bulmak büyük bir problemdir.

Güneş enerjisi, ısı enerjisi, titreşim enerjisi gibi yeşil çevresel enerji kaynaklarından enerji harmanlama, bahsi geçen cihazlara güç sağlamak için son zamanlarda önem kazanmıştır. Bu kaynakların yanı sıra, radyo frekansındaki (RF) dalgalardan enerji harmanlama da, bu dalgaların devamlı bulunmasından dolayı olası bir aday olarak ortaya çıkmaktadır. Ancak RF enerji harmanlama sistemlerinin tasarmı ve gerçeklenmesi gibi önemli zorlukların aşılması gerekmektedir. Bu tezde 900 MHz ve 1800 MHz'de çalışan hücresel telefon baz istasyonlarından RF enerji harmanlayan sistemlerin tasarımı ve analizi sunulmaktadır. Ayrıca tezin yenilikçi bir yönü de, telsiz kanalın toplam harmanlanan enerjiye gerçek zamandaki etkisinin araştırılmasıdır. Bunlara ek olarak, bir algılayıcı ağ düğümünün farklı işleyiş durumları altında ne kadar enerji tükettiği tartışılmıştır. Bunun için en son nesil Berkeley mote düğümlerinden olan OpenMote donanımı kullanılarak deneyler yapılmış, algılama, paket gönderimi ve alımı gibi farklı işleyiş durumları altında enerji tüketimi ölçülmüştür.

ACKNOWLEDGEMENTS

I would like to express my immense gratitude to my advisor, Asst. Prof. Ali Özer Ercan. I owe my entire thesis to his continuous support, encouragement and careful assessment which always enlightened my path. He always helped me in any financial and academic issue. He has always put his full effort to make my work better with his insightful comments and feedback. His broad knowledge in diverse field of science always inspired me. Despite of his busy schedule he always finds time for our meetings and discussions.

This work has been supported by the Scientific and Technological Research Council of Turkey (TÜBİTAK) under BIDEB-2215 graduate scholarship programme for international students and under Grant No. 114E739. TÜBİTAK's support has definitely allowed me to contribute significantly to Turkey's goal of international cooperation in scientific and technological development. I have a firm belief that, without the support of TÜBİTAK scholarship I would never be able to pursue my graduate studies in Turkey.

I would like to thank the members of my committee Assoc. Prof. Onur Kaya and Asst. Prof. Ahmet Tekin for accepting our request and for providing their worthy comments and feedback on my thesis draft.

I owe my gratitude to the faculty members of Özyeğin University who always been very cooperative and motivational for me. They enhanced my knowledge with there up-to date knowledge and skills. I would like to thank Dr. Engin Zeydan for his support and motivation in research activities. I learned many concepts of RF/microwave from Prof. Şahabettin Taha İmeci, so I would like to thank him for enhancing my knowledge.

I would like to express my special thanks to my colleague Syeda Wajiha Munir for her support and encouragement throughout the project. She is always ready to help and share her knowledge. I am thankful for her constant availability during the project and her tolerance in good and bad times.

I wish to thank the Özyeğin University, WISER Lab for providing good facilities and atmosphere for research activities. I would also like to thank other members of my Lab who have always been very supportive and kind to me.

Last but not the least, I would like express my deepest gratitude to my parents, sister and brother. Without their support, encouragement and never ending love I would never be able to accomplish any goal. I am extremely fortuitous and honoured to have them in my life. The prayers and encouragement of my mother played a great role in completing my degree. I would like to dedicate this thesis to my father (may his soul rest in peace) who always wanted to see me in a position of high esteem.

TABLE OF CONTENTS

LIST OF TABLES

LIST OF FIGURES

CHAPTER I

INTRODUCTION

1.1 Motivation

In the recent years, there has been rapid growth of low power wireless devices, such as wireless sensor networks (WSNs) and Internet of Things (IoT). These sensors require low power but since they are deployed in large numbers, therefore the demand of energy supply for perpetual operation of such sensors is also increasing. Figure 1 shows that with the evolution of technology, the wireless devices are increasing exponentially.

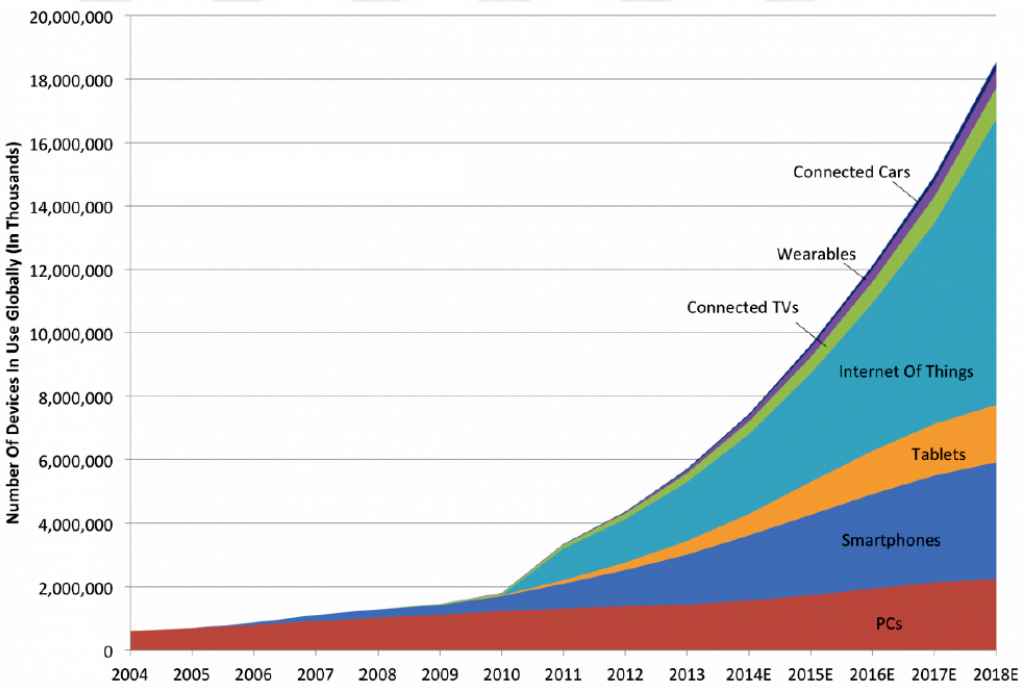

Figure 1: The evolution of wireless applications and technologies [1].

However, in comparison the evolution of battery technologies is not yet capable to meet the energy demand of these ever-growing wireless applications. Therefore,

there exists a huge gap between the energy demand of the wireless devices and the energy density resulting from the development in battery technology. This poses a lot of questions to the researchers that how to deal with such a situation, how to improve the battery life and ultimately the satisfaction of customer with minimum charging interruptions.

Conventionally, these devices were powered by batteries, which have limited life time and were needed to be replaced/recharged manually once the energy is consumed. Moreover in practice, battery maintenance and replacement becomes unsuitable, when wireless network are deployed at hard-to-reach places (e.g., remote rural areas, concrete structures) or even infeasible for some applications (e.g., implanted within human body) [2]. Therefore, to find another source of energy that can sustain sensor node operations, is a major challenge.

The concept of energy harvesting has gained much importance as an alternate source of battery reliance. Many ambient green energy sources are available for harvesting energy such as, solar, thermal, vibrational and RF. Out of these green sources of energy, RF energy harvesting has been significantly used in academics and R&D for charging the low-power devices. RF signals that are extensively available in environment are captured through efficient receiving antenna and are converted to usable DC power. With the substantial growth of mobile communication services due to the introduction of 4G/5G technologies, and the explosive growth in Internet on commercial and personal basis, focus our attention towards harvesting energy from cellular base stations. As the technology and industry grow, the power sources will grow too. Therefore, it is logical to address those sources for RF energy harvesting that are more likely to grow with the development of technology.

1.2 Thesis Contribution and Organization

The presented work in this thesis is twofold; first part demonstrates the design and analysis of RF energy harvesting from cellular base stations operating at 900 MHz and 1800 MHz. The proposed architecture of RF energy harvesting system consisting of receiving antenna, matching network, voltage rectifier and storage circuit, has been designed and analyzed in detail.

- In the previous research work, the effect of wireless channel, effect of different geographic environments and the effect of source power on the harvested energy has not been considered. In this work, wireless channel and transmitting source has been introduced in the simulation setup, which is the novel aspect of this thesis. These parameters helps to investigate the effect of wireless channel on harvested energy under different shadowing conditions. Integration of transmitting source with the harvesting circuit helps to understand the effect of source power and the effect of distance on the total harvested power.

- In comparison to the past work, that only considered the single frequency band for energy harvesting, this work focuses on the design of dual band energy harvesting system that utilizes Inverted-F-Antenna (IFA), which can simultaneously harvest from dual frequencies of cellular base stations.

Secondly, the application of RF energy harvesting in WSNs has been demonstrated, which has become a potential solution to energize the low power wireless devices, such as autonomous sensor nodes. Major energy consumption of a sensor node is during sensing, transmission and reception of data. To supply energy through a battery, that needs to be physically recharged or replaced, is not an efficient solution. The other approach is that nodes can harvest RF energy from the environment for their required operations.

- Our research aims to report the power consumption of sensor node under different states. In this regard, we have used OpenMote hardware, the latest generation of Berkeley motes and practical experiments are performed to calculate the power consumption under different states. Moreover, power consumption and harvested power has been compared and analyzed, which reveals that designed system is efficient enough to energize the OpenMote for sensing operation.

Chapter-2 presents the literature review, in which the possible sources of energy harvesting are discussed and their power densities have been compared. It has also been explained that despite of having lowest power density as compared to other natural sources of energy, RF energy harvesting is still preferable for charging the low power devices because of its several advantages.

Chapter-3 includes the design and analysis of dual band WLAN microstrip patch antenna for harvesting energy from both 2.4 GHz and 5.8 GHz. Moreover, Inverted-F-Antenna (IFA) has been designed for energy harvesting from cellular base station frequencies operating at 900 MHz and 1800 MHz simultaneously.

Chapter-4 focuses on design and analysis of RF energy harvesting from cellular base stations. To ensure maximum power transfer from the receiving antenna to the voltage rectifier block, two separate LC-impedance matching networks are designed. The designed harvesting circuit utilizes a 5-stage voltage rectifier consisting of HSMS-2850 schottky diodes. Different parameters are varied to investigate their effects on total output power and the efficiency of the system.

Chapter-5 is based on the experiments with OpenMote kits to determine the power consumption demand of these sensor nodes. Initially, the OpenMote hardware is explained in detail along with its related interfaces. Experiments have been performed on the motes to measure the current consumption during different operations. The effect of distance on power consumption of OpenMote has also been shown during transmission and reception of data and the results are recorded.

CHAPTER II

RF ENERGY HARVESTING SURVEY

2.1 Sources of Energy Harvesting

This section provides the brief overview of available sources for energy harvesting and their characteristics. Energy can be harvested from different sources such as wind, solar, vibrational, thermal and RF, etc. Figure 2 shows most commonly used sources for energy harvesting [3].

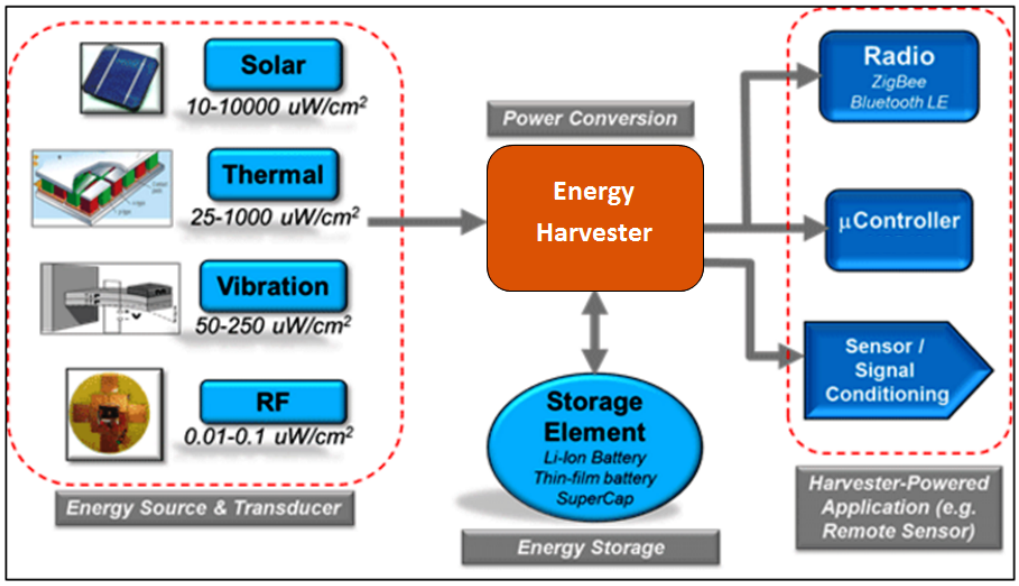

Figure 2: Potential alternatives for energy harvesting [3].

In solar energy harvesting, the ambient solar energy is converted to the electrical energy. The nuclear reactions that occurs inside the sun generates the photons, which reaches the earth in the form of electromagnetic waves. These electromagnetic waves are converted to the electrical energy using photovoltaic (PV) panels [4]. Solar energy harvesting is not a new concepts as the solar calculators and streets lights with solar panels are commonly seen since many years ago. Due to its high power

density, typically in a range of ($10\ \mu W/cm^2 \sim 10\ mW/cm^2$) a huge amount of research work has been done on micro-solar PV and hardware design for energy harvesting to make efficient use of solar energy. However, there are many factors that need to be accounted for practical implementation of solar energy harvesting, as the efficiency of solar harvesting is almost negligible during night time and cloudy/rainy weather.

Thermal energy is another major source for energy harvesting, and the power densities usually lies in the range of ($20\ \mu W/cm^2 \sim 1\ mW/cm^2$). In thermal energy harvesting, the heat is converted to usable electric energy; for example, the heat generated from industrial machines, home gadgets, auto vehicles and human body. Thermal wrist-watch is a practical example of this technique, in which the clock moment occurs due to the heat generated by the body [4].

Energy harvesting from vibrations, also known as piezoelectric energy harvesting gained much attention in the recent years, which provides a promising solution to power the sensor nodes. This type of energy harvesting is usually beneficial in those areas, which have enough vibration activities; such as railway/subways tracks, bridges, etc., [5] and the energy harvested is usually falls in the range of ($50\ \mu W/cm^2 \sim 0.25\ mW/cm^2$)

2.2 Radio Frequency Based Energy Harvesting

RF energy harvesting is a technique, in which energy is harvested from abundantly available RF signals in the surrounding atmosphere. In RF energy harvesting, signals from 3 kHz to 300 GHz are used as a medium to carry signals in the form electromagnetic (EM) radiations [2]. These signals are captured by an efficient antenna which is connected to hardware called energy harvester, which converts the received signals into functional DC power. Thus, this method of energy scavenging provides an efficient solution to empower low-power wireless applications. The most commonly used sources for energy harvesting from the RF spectrum are high power FM/AM radio

broadcast stations, analog/digital TV broadcasting towers, cellular base stations and WLAN access points [2]. The energy harvested from RF signals is typically in a range of ($0.01\ \mu W/cm^2 \sim 0.1\ \mu W/cm^2$), which is significantly low as compared to power densities of other energy sources. Despite of low power density, RF energy harvesting can be promising solution to power the energy-constrained wireless network with careful design and analysis of receiving antenna and harvesting circuitry. RF energy harvesting is a potential candidate for scavenging energy due to several advantages: RF energy is available all the times irrespective of geographical area and weather conditions, etc., which must be considered during harvesting from other energy sources such as, solar or wind energy harvesting. Another useful feature of RF signals, is that they can pass through water, glass, plastic, etc., therefore, harvesting device can be placed at such places which are not exposed to direct sunlight and consequently, RF energy harvesting can be the only possibility. The RF sources are mainly categorize into two types, i.e., Intended (Dedicated sources) and Non-intended (Ambient sources) [5].

2.2.1 Dedicated RF Sources

The dedicated RF sources include specially designed powercast RF transmitters which have particular operating parameters. For example, in [2] a powercast transmitter which operates at 915 MHz, with 1 W or 3 W transmit power is a dedicated RF source. Moreover, in research P1100 powercast has been used, which is highly efficient RF energy harvesting device. Similarly, powercast TX91501 as a RF power transmitter was specially designed for P2110 or P1110 power harvester receiver in energy harvesting network [2]. It transmits the power in the form of Dynamic Sequence Spread Spectrum (DSSS) and data in the Amplitude shift keying modulation (ASK); therefore, such types of sources are more reliable and uninterrupted but they are highly distance dependent.

2.2.2 Ambient RF Sources

Ambient RF sources refers to signals radiated from the wireless telecommunication services, such as cellular systems, mobile devices and WLAN or from public broadcasting systems, e.g., TV and radio [2]. They are not intended for RF energy harvesting systems, but they are present in the free environment and they may get wasted in the form of heat, if not captured by their respective receivers. The transmitted power of ambient RF sources varies significantly, from around 10^6 W for TV tower, to about 10 W for cellular and RFID systems.

2.2.3 Existing Research on RF Energy Harvesting

With the ever growing trend of wireless devices used globally, the need to adopt the green, efficient and inexpensive strategies is of significant importance. In this regard, RF energy harvesting becomes an interesting research topic in the academic and R&D environment. In this field, remarkable work has been done ranging from efficient antenna design to scavenge enough RF signals to power the devices like wireless sensor nodes. More specifically, energy harvesting from cellular base stations and WLAN access points have gained much attention, as their signals are omnipresent [6]. In today's wireless communication systems, development of multiple frequency bands has provided the multi-band rectennas structures for RF energy harvesting, which is quiet useful. In [6] and [7] dual band RF energy harvesting system along with efficient receiving antenna for GSM and WLAN signals are designed and analyzed respectively. Dual-band circularly polarized monopole antenna for RF energy harvesting in GSM (935-960 MHZ, 1810-1880 MHz) bands has been presented in [8]. In [9], RF energy harvesting system along with the dual-band microstrip patch antenna has been designed to power the wireless sensor nodes. The antenna simultaneously operates at 1.8 GHz and 2.4 GHz ISM band. The experimental setup of RF energy harvesting system from cellular base stations is presented in [10] and [11]. In [12]

and [13] energy harvesting from 2.45 GHz indoor Wi-Fi signals has been discussed. Experimental results of RF energy harvesting from TV towers has been discussed in [14], where the designed system utilizes a broadband log periodic antenna. The system harvests 60 μW of energy at the output of 4-stage voltage rectifier and at a distance of 4.1 km from the TV tower. In [15], the novel energy harvesting approaches are discussed for Information and Communication Technologies (ICT) applications, where various RF frequencies have been tested and evaluated in terms of efficiency and for different environments.

Table 1: Reported Experimental data on RF energy harvesting.

Source	*SourcePower*	*Frequency*	*Distance*	*EnergyHarvested*
GSM900 [16]		935-960 MHz	25-100 m	$10^{-3} - 10^{-1} \mu W/cm^2$
GSM1800 [16]		1805.2-1879.8 MHz	25-100 m	$10^{-3} - 10^{-1} \mu W/cm^2$
GSM [17]	100 W		100 m 500 m 1000 m	800 $\mu W/m^2$ 32 $\mu W/m^2$ 8 $\mu W/m^2$
Wi-Fi [17]	1 W		1 m 5 m 10 m	80 $\mu W/m^2$ 3.2 $\mu W/m^2$ 0.8 $\mu W/m^2$
Powercast Transmitter (TX91501) [18]	3W 3W	915 MHz 915 MHz	5 m 11 m	189 μW 1 μW

2.3 Applications of RF energy harvesting in WSNs

In RF harvesting scheme, the power densities are usually not too high, and the amount of energy harvested is in the order of micro-watts. This small amount of energy can be sufficient to energize the low power devices such as WSNs. Therefore, one of the widely used application of RF energy harvesting is to power the autonomous WSNs, and such type of wireless networks are known as Energy Harvesting WSNs (EH-WSNs) [4]. In order to design an efficient harvesting system, which is able to power the sensor node during its different operations; it is necessary to determine the current consumption of a device during its different operations such as sensing, transmission/reception etc. In this regard, extensive research work has been done in order to calculate the energy consumption of a typical sensor node. Different low-power platforms are used in research for experimental purpose in which the most popular are, MICA family mote by Crossbow, TelosB which include Tmote Sky, Zolertia Z1 mote and IRIS mote [19]. In [20], modeling of energy consumption based on the current drawn under different operations of 802.15.4 Zigbee sensor motes has been presented. Similarly, current consumption of the Texas Instruments eZ430-RF2480 Kit has been measured under different states. A realistic energy consumption model has been detailed in [21], in which the Guidance and Inertial Navigation Assistant (GINA) mote and OpenMote has been used in experiments to measure their current consumption in idle, sleep and during transmission and reception modes.

Another interesting application of RF energy harvesting is in RFID, which has been extensively investigated in research [2]. RFID is widely used in automatic identification and tracking of the tags; whereas, RF energy harvesting scheme can be used to increase the lifetime of the conventional RFID tags. Therefore, RFID tags instead of relying on the battery or RFID reader, can harvest RF energy in order to perform their required tasks. Additionally, a wide range of low power devices; such as cell phones, electronic watches, wireless keyboards, mouse and MP3 players etc., can be

powered using RF energy harvesting technique. Since the amount of energy harvested from this scheme is usually in the range of micro-watts, and most of these low power devices consume energy in a range of micro-watts to milli-watts; therefore, RF energy harvesting is the reliable option for charging such devices. In [22], wireless cell-phone battery charging using RF energy harvesting technique, has been discussed in detail and the charging of phone battery has been practically demonstrated.

CHAPTER III

DESIGN OF DUAL-BAND ANTENNAS FOR WLAN AND CELLULAR ENERGY HARVESTING

This chapter focuses on the dual band antenna design for both cellular and Wi-Fi energy harvesting system. The introduction of 4G/5G cellular technologies and the increased utilization of Internet services leads to the corresponding increase of their sources in the environment. Moreover, energy harvesting from cellular base stations and WLAN access points have been significantly used, as their signals are omnipresent [7]. Therefore, the presented work shows the design of energy harvesting antennas for these two ever growing potential candidates of RF signals.

The antenna is the most important and key element of RF energy harvesting system, as it captures the RF signals and convert them to usable DC power [23]. The amount of harvested energy is greatly affected by the characteristics of receiving antenna; therefore a suitable harvesting antenna is very important in this respect. In past few years, different types of antennas have been proposed for RF energy harvesting such as, dipoles, Yagi-Uda, microstrip patch, monopole, loop, spiral, coplanar patch and Inverted-F-antennas (IFA) [24]. The antenna can be designed to operate on either single frequency or multiple frequency bands, in which the device can simultaneously harvest from a single or multiple sources [2]. It has been explained in [24], that single band antenna is not much efficient for RF energy harvesting systems; therefore, the development of the multi-band antennas structures are widely preferred.

3.1 Microstrip Patch Antenna for WLAN Frequencies

Microstrip patch antennas are widely used in many satellite and mobile communication applications due to their low profile, light weight, easy fabrication and installation. As from name, microstrip patch antenna usually consists of radiating patch of certain frequency on one side of the dielectric substrate and a ground plane on the other side of substrate [23]. Our proposed microstrip patch antenna, which has been published in [25] can simultaneously harvest from both 2.4 GHz and 5.8 GHz frequency bands.

3.1.1 Design Methodology

The antenna size is characterized by its length, width, and height (and is fed by feed line and is followed by a ground plane) and generally microstrip antennas are $\frac{1}{2}\lambda$ structures. The geometry of the proposed antenna shown in Figure 3, has been designed on ADS and Sonnet Suites software using FR4 substrate. Dual resonating

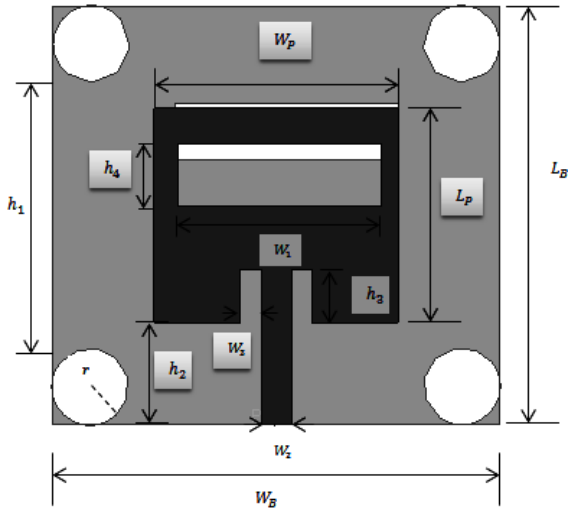

Figure 3: Dual-band antenna designed for WLAN RF energy harvesting.

frequencies are obtained by introducing a rectangular slot in the top and bottom patch of the design. The physical dimensions of patch antenna can be calculated

using the equations mentioned in [26]. The length and width of patch antenna is modeled according to the respective design frequency. In this regard, the width of top patch is given by:

$$W = \frac{C}{2f_o\sqrt{\frac{\epsilon_r+1}{2}}} \tag{1}$$

Whereas, the actual length of radiating patch can be calculated using following equation:

$$f = \frac{C}{2L\sqrt{\epsilon_r}} \tag{2}$$

In the above mentioned equations, ϵ_r is the relative permittivity of the grounded FR4 substrate. i.e. 4.4, which has a considerable effect on dimensions and overall performance of antenna [26]. Whereas, f is the resonating frequency of designed antenna, C is the speed of light and L is the patch length of antenna.

The dimensions of the ground plane are also of significant importance because they control the return loss at the designed frequency band. The corresponding dimensions of ground plane can be calculated from actual length (L) and width (W) of top patch of antenna as follows [26]:

$$L_g = 6h + L \tag{3}$$

$$W_g = 6h + W \tag{4}$$

The calculated physical parameters of proposed antenna have been optimized to obtain maximum return loss and bandwidth at both resonating frequencies. The corresponding calculated dimensions (mm) are listed in Table. II, which provide maximum efficiency in terms of directivity and return loss.

Table 2: Physical Parameters of Dual Band Microstrip Patch Antenna.

Parameters	L_P	W_P	L_B	W_B	W_1	W_2	W_3	W_4	h_1	h_2	h_3	h_4	h_5	r
Dimensions(mm)	21	24	41	44	20	3	2	22	26	10	5.2	5.98	5.5	3.75

3.1.2 Simulation Results

The designed antenna has been evaluated using ADS and Sonnet suites simulators and corresponding results have been recorded. Figure 4 shows the simulated results of the proposed antenna, it is clear that 10 dB reflection coefficient at 2.4 GHz is almost -25 dB; whereas at 5.8 GHz, the reflection coefficient is as low as -35 dB. The simulation results shows that the designed antenna only receives dual-band WLAN frequencies and attenuates the rest of unwanted frequencies.

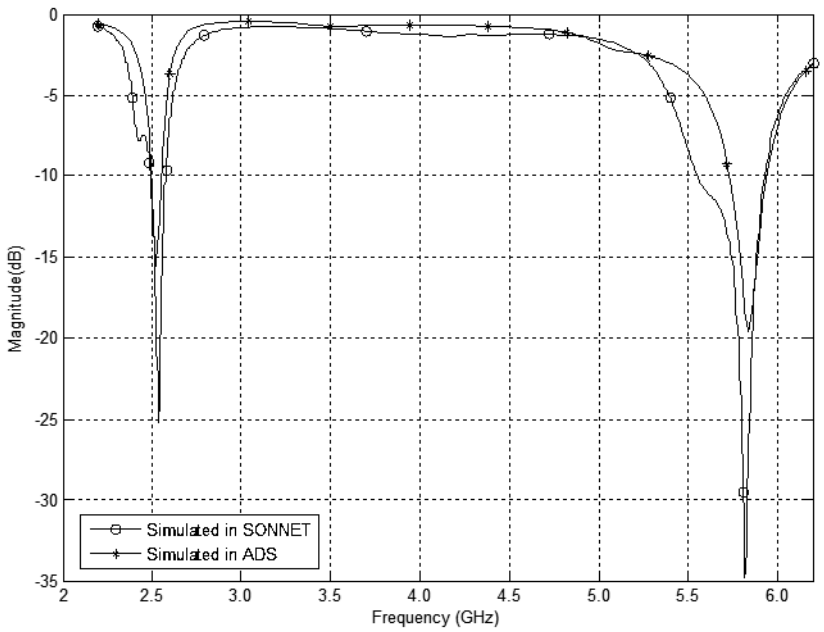

Figure 4: Reflection coefficient of proposed microstrip patch antenna.

3.2 Inverted-F-Antenna for Cellular Frequencies

In this section, the design and analysis of a Inverted-F-Antenna (IFA), has been presented as shown in Figure 5. This type of antenna is widely used in many wireless communication applications such as; cellular, Wi-Fi and Bluetooth communication in mobile phones [27]. An important feature of this antenna is the compact $\frac{\lambda}{4}$ resonant length, which makes it easy to fabricate and thus offers an omnidirectional radiation

pattern with good efficiency [28]. Moreover, this antenna can be mounted with the other RF components on the same printed circuit board (PCB) using microstrip transmission lines.

3.2.1 Antenna Geometry

The dual-band IF-antenna is designed to harvest energy from dual frequencies of cellular base stations i.e. 900 MHz and 1800 MHz. The designed antenna is simulated on ADS software using Rogers 4003 substrate with a thickness of 0.813 mm, a dielectric constant (ϵ_r) of 3.55, and a loss tangent (TanD) of 0.0027. Figure 5 shows the top and bottom view of receiving antenna, having two arms; the upper arm operates at 900 MHz, while the lower arm operates at 1800 MHz and is integrated inside the upper arm. A microstrip feed line for excitation is provided to the 1800 MHz arm having

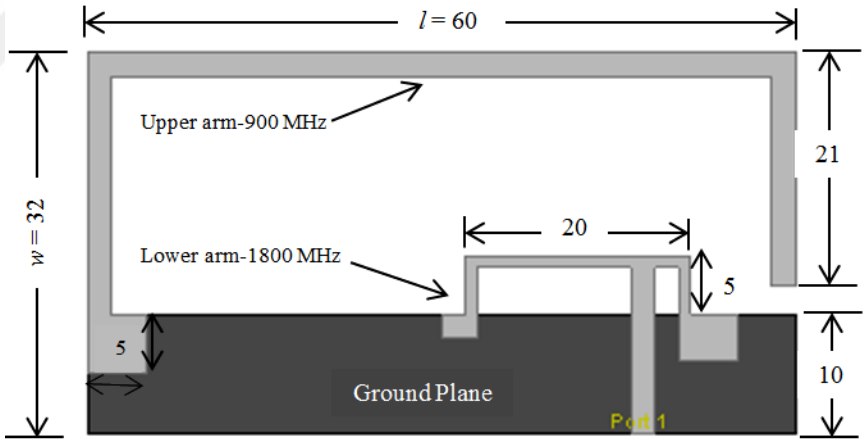

Figure 5: Dual-band antenna designed for cellular energy harvesting.

an impedance of 50 Ω. Whereas, the combination of the 1800 MHz arm and the feeding line act as an indirect source for the 900 MHz arm, as this arm is fed through the mutual coupling between itself and 1800 MHz arm. The physical dimensions of IF-antenna have been calculated using following equations [29]:

$$f_{r1} = \frac{C}{4(H + L_1 + W_1)\sqrt{\epsilon_r}} \tag{5}$$

$$f_{r2} = \frac{C}{4(L_2 + W_2)\sqrt{\epsilon_r}} \tag{6}$$

Where, ϵ_r is the relative permittivity of the substrate, H is the height in reference to ground plane and f_{r1}, f_{r2} are the corresponding resonating frequencies. C is the speed of light, L_1, W_1 and L_2, W_2 are the lengths and corresponding widths of upper and lower arms respectively. The overall dimensions of upper arm is 60×32 mm and the ground plane of the antenna has a rectangular patch of dimensions 60×10 mm.

3.2.2 Simulated Results

Figure 6 shows the simulated result of antenna, it can be seen that the antenna has two operating bands around the center frequencies of 900 MHz and 1800 MHz. Clear

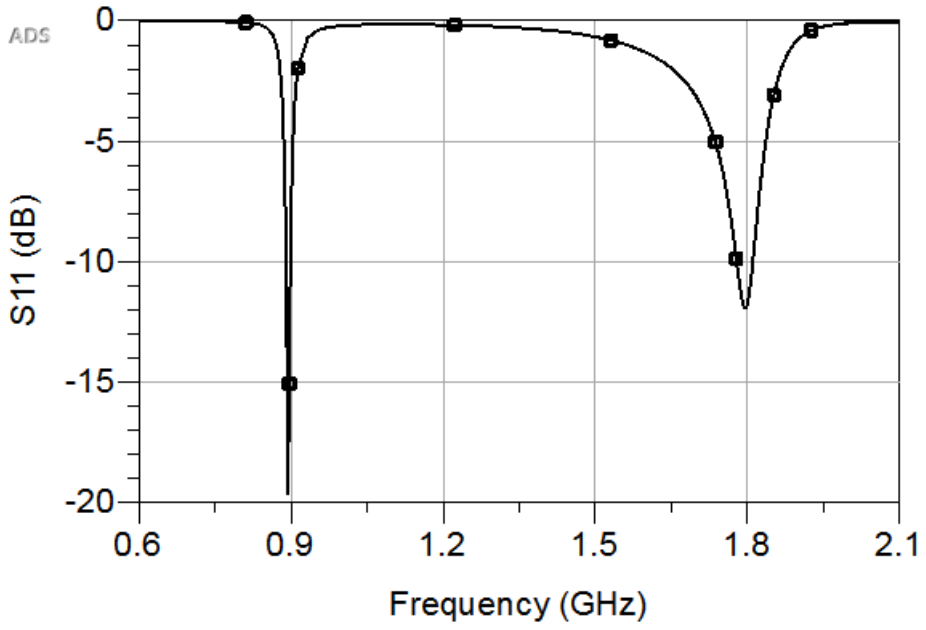

Figure 6: Input reflection coefficient (S11) of the inverted-F-antenna.

resonances are produced at both the frequencies, which ensures the maximum power delivery with reflection coefficient as low as -20 dB at 900 MHz and -13 dB at 1800 MHz respectively.

3.3 Discussion

The proposed antennas can be used for RF energy harvesting from dual frequency bands of WLAN and cellular base stations. Our ultimate goal is to integrate the designed antennas with their respective energy harvesting system. In this regard, we have designed dual-band WLAN energy harvesting system, which has utilized the presented WLAN microstrip patch antenna and corresponding work has been published in [30]. Whereas, energy harvesting system for cellular base stations, which utilizes dual-band IFA, will be discussed and analyzed in the next chapter.

CHAPTER IV

ENERGY HARVESTING FROM CELLULAR BASE STATIONS

Radio Frequency (RF) energy harvesting also known as RF energy scavenging is a promising solution to energize the energy-constrained wireless devices. Energy can be harvested either from the surrounding environment or dedicated RF sources. In RF energy harvesting, signals from 3 kHz to 300 GHz can be used as a medium to carry energy in the form of EM radiations. The most commonly used sources for energy harvesting from the RF spectrum are high power FM/AM radio broadcast stations, analog/digital TV broadcasting towers, cellular base stations and WLAN access points.

For employing RF energy harvesting, now a days the most interesting systems to be explored are 3G and 4G cellular base stations. These systems are omnipresent and ubiquitously available in an urban area, as they propagate well both in the indoor and outdoor environments. Moreover, such frequency bands allow the dimensions of receiving antennas in the order of 10-50 cm^2 [16]. Therefore, cellular base stations can be one of the potential candidate for RF energy harvesting.

4.1 General Architecture of RF Energy Harvesting System

The general architecture of RF energy harvesting system has been shown in Figure 7. The most important component of energy harvester is the receiving antenna, which captures the ambient RF signals of a particular frequency band from transmitting source via wireless channel and converts these signals to AC voltages [17]. The matching network, composed of capacitive and inductive elements ensures the

maximum power delivery from receiving antenna to the voltage rectifier by reducing the transmission loss. Matching network has AC type voltage at the output, therefore the voltage rectifier is used to convert this voltage into usable DC power. The obtained power is either directly supplied to energize the low power device or stored in the energy storage unit. The storage circuit allows uninterrupted power delivery to the load and serve as a backup reserve, when external energy is not available. The detail of each sub-component is mentioned in the following subsections.

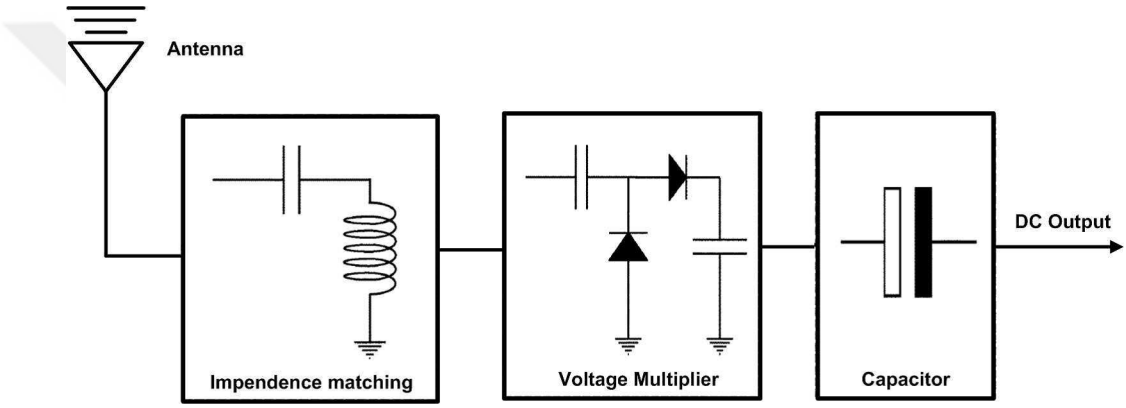

Figure 7: General architecture of RF energy harvesting [2].

4.1.1 Receiving Antenna

The key element of RF energy harvesting system is receiving antenna, which captures the RF signals of particular frequency via wireless channel and convert them to functional DC power by a device known as RF energy harvester. Dual-band Inverted-F-antenna will be used in the proposed energy harvesting system, which scavenges energy from dual frequencies of cellular base stations. i.e. 900 MHz and 1800 MHz. The antenna geometry and the detailed design methodology has been explained in the previous chapter.

4.1.2 Impedance Matching Network

Another important consideration in the design of RF energy harvesting circuit is impedance matching. It reduces the transmission loss between antenna and the rectifier, thus increases the input voltage of the voltage rectifier. According to the maximum power transfer theorem for DC circuits, the maximum power will be transferred from a source to its load, if the load resistance is equal to the source resistance. In AC, the same theorem states that the maximum transfer of power from a source to its load occurs when the load impedance (Z_L) is equal to the complex conjugate of the source impedance (Z_S) [31].

Different types of matching configurations are available for RF energy harvesting, such as transformer, a shunt inductor and LC matching network. The most frequently used matching network for energy harvesting is LC matching scheme, which is usually a combination of capacitor and inductor. It is preferable over other matching configurations, as it provides higher peak voltage to the rectifier and offers better efficiency especially, when the available power at the antenna to be delivered is low [31]. Figure 8 shows the four different configurations of LC matching network with different orientation of capacitors and inductors. Figure 8 (a) and (c) are in low-

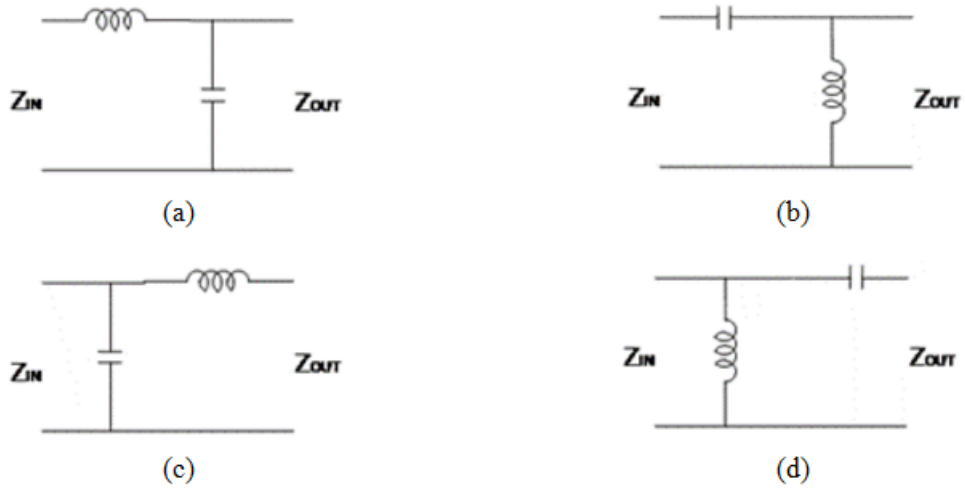

Figure 8: Different configurations of LC matching network.

pass configuration LC network, whereas Figure 8 (b) and (d) are LC networks with high-pass configurations.

Matching network depends upon the operating frequency of RF source, therefore; two separate matching networks are designed for dual frequencies of cellular band. In the presented work, ADS smith chart utility has been used to obtain two different LC matching networks for dual frequency bands with optimal values of inductor and capacitor, such that high RF-DC conversion efficiency is achieved. The orientation of capacitor and inductor shown in the Figure 8 (a) has been used in our matching network design, which matches the input voltage to output voltage as shown in Figure 9. It provides maximum return loss at both frequencies. Moreover, the source and load impedance are also perfectly matched with this configuration.

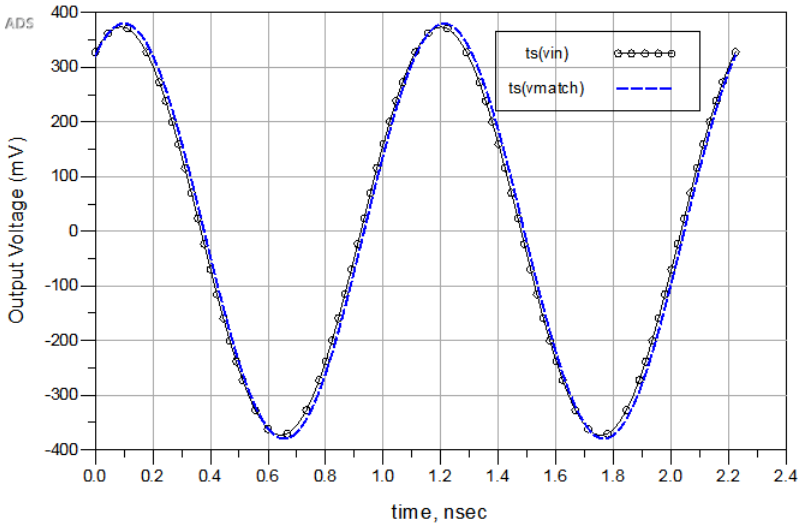

Figure 9: Matched output voltage after LC-impedance matching.

4.1.3 Voltage Rectifier Design

RF signals are converted into DC voltage at the given frequency band to energize the low power devices/circuits. The voltage rectifier is usually composed of diodes and capacitors. The output of the matching network has AC type voltage, therefore

voltage rectifier is used which converts the signal to usable DC voltage. Moreover, if multiple stages of the voltage rectifier are cascaded together, the output voltage can be increased. Various types and topologies of the voltage rectifier have been used in research depending upon the design and the application [32].

4.1.3.1 Greinacher Voltage Rectifier

In the presented work, the Greinacher voltage rectifier has been utilized in designing RF energy harvesting system. This rectifier works on the principle of peak or envelop detection by removing the ripples and preserving the output voltage peaks. The single stage voltage rectifier is shown the Figure 10, which has two sections; each consists of a diode and a capacitor for rectification. The capacitors C_1 and C_2 are input capacitor and charging capacitor respectively; whereas, the diode D_2 is connected in the forward bias configuration and D_1 is connected in reverse bias configuration, such that they convert the positive and negative half cycles of the input signal to a DC voltage. During the positive half cycle, the RF input signal is rectified followed by the negative half of the input cycle. Whereas, the voltage stored on the input capacitor during first half cycle is transferred to the charging capacitor during the next half cycle of the input signal [32]. This type of voltage rectifier is also known as voltage doubler since the voltage obtained at output of the rectifier is usually twice of the input voltage.

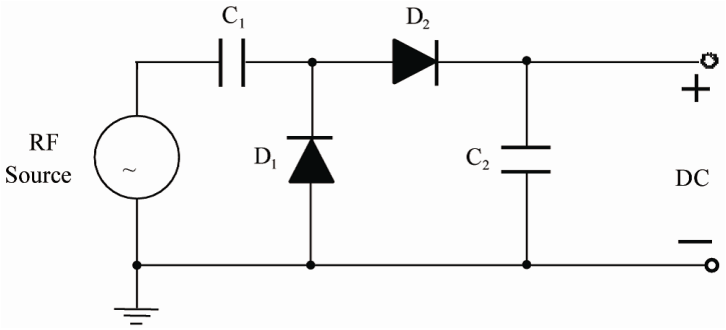

Figure 10: A single stage voltage rectifier.

4.1.3.2 Characteristics of HSMS-2850 Schottky Diode

The diode is the key element in the voltage rectifier circuit, which offers least resistance to the flow of current in one direction whereas, offers high resistance to the current flow in other direction. Thus, it converts the AC signal to DC current and voltages, which can be used further to energize the low power devices. Therefore, such diodes should be selected which have high conversion efficiency and low substrate leakage.

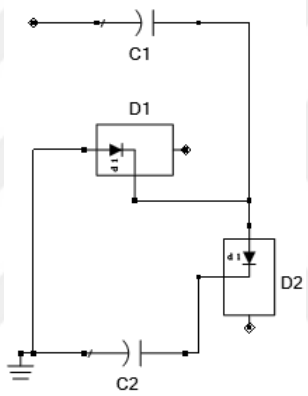

Figure 11: A single stage voltage rectifier with schottky diodes.

In the presented work, silicon based HSMS-2850 Schottky diode provided by the ADS Agilent libraries has been used in the design of voltage rectifier as shown in Figure 11. It has threshold voltage of 250 mV and diode capacitance of 0.18 pF. The main advantage of such type of diodes is their ability to provide low forward voltage, low substrate leakage and unidirectional flow of current [32].

4.1.3.3 Five Stage Voltage Multiplier

The output voltage at the first stage of the rectifier is usually too low for energizing a low power device and the conversion efficiency is also not very high. Therefore, for designing RF energy harvesting system multiple stages of voltage rectifier are connected in series one after the other stage, so as to achieve sufficient amount of

voltage at the output to power the particular device [33]. The selection of number of stages is a crucial task in designing the system. Optimal number of stages should be added to the system because parasitic loss of non-linear devices increase by increasing number of stages, which effects the overall performance and efficiency of a system [34]. Five stages have been used in the designed circuit which provides enough voltage at the output that can be used to power the required WSN applications. Increase in voltage is directly proportional the number of stages, but there reaches a point where increase in voltage becomes negligible by adding extra stages in the design or the voltage may even decreases; thus, making it necessary to choose such number of stages which can provide sufficient voltage to intended low power device.

4.1.4 Storage Circuit

The storage circuit is of significant importance in RF energy harvesting system because it ensures uninterrupted power delivery to the load and serves as a backup reserve, when RF signals are unavailable [34]. The circuit includes a capacitor across the load to store and provide DC output voltage. The output is not a good DC signal without a capacitor across the load, therefore a storage capacitor which can store sufficient amount of charge is necessary for the design. In addition to the capacitor, an optimized load resistor is connected in parallel to the capacitor. Without the load resistor, voltage would look like a DC signal and held indefinitely on the capacitor [32].

4.2 Design and Analysis of Overall RF Energy Harvesting System

This section includes the detailed analysis of the designed system, which has been designed on ADS Agilent software. Figure 12 shows integrated matching network and voltage rectifier for the receiving side of RF energy harvesting system. Coupler is used to combine antenna model with voltage rectifier after impedance matching.

According to research in [32], the stage capacitors with same values have better results as compared to the capacitors of different values in each succeeding stage capacitor, with half of the previous stage capacitor value. Therefore, the stage capacitors with equal values are used in our design for all the five stages.

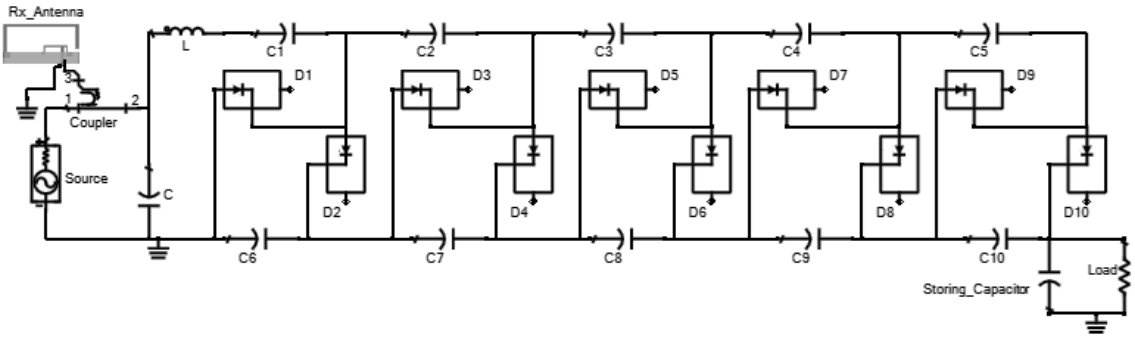

Figure 12: The overall designed circuit for RF energy harvesting.

4.2.1 Effect of Rectifier Stages

The number of rectifier stages has a major influence on the output power of the energy harvesting circuit, as described in the previous section. Figure 13 shows that output power is directly proportional to the number of stages. ADS parameter sweep for an input power of -5 dBm to 25 dBm has been used for the simulation and the number of rectifier stages are varied from 1 to 5 stages. It can be seen that, the power increases linearly with addition of each stage. For an input received power of 15 dBm and at 900 MHz frequency, the circuit provides an output power of 19 mW and 24 mW at the output of 4-stage and 5-stage voltage rectifier respectively.

Similarly, the effect of rectifier stages on the output power at 1800 MHz can be seen from Figure 14. It can be noticed from Figure 13 and Figure 14 that for the constant received power, the power obtained at higher frequency i.e. 1800 MHz is lower than the power obtained at 900 MHz. It is due to the fact, that high frequencies are more vulnerable to attenuation and absorption; therefore, power obtained at low

frequency is relatively high. For example, at an input received power of 15 dBm and for 5-stage rectifier, the output power at 900 MHz is almost 24 mW, whereas at 1800 MHz the obtained power is 18 mW across 10 kΩ load.

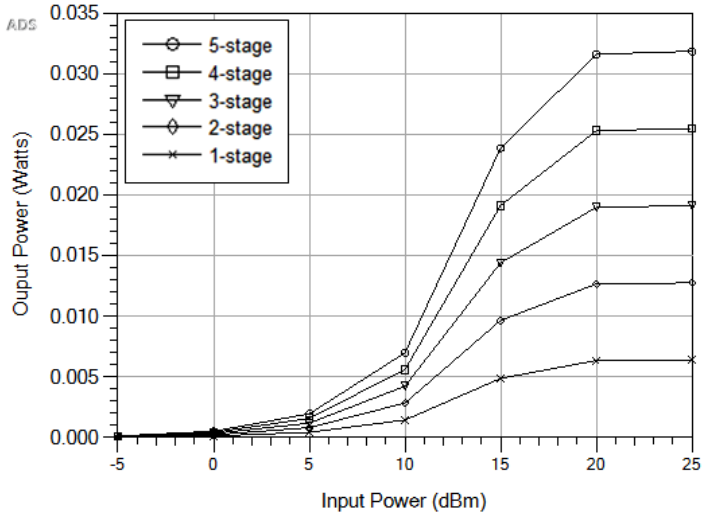

Figure 13: Effect of rectifier stages on output power at 900 MHz.

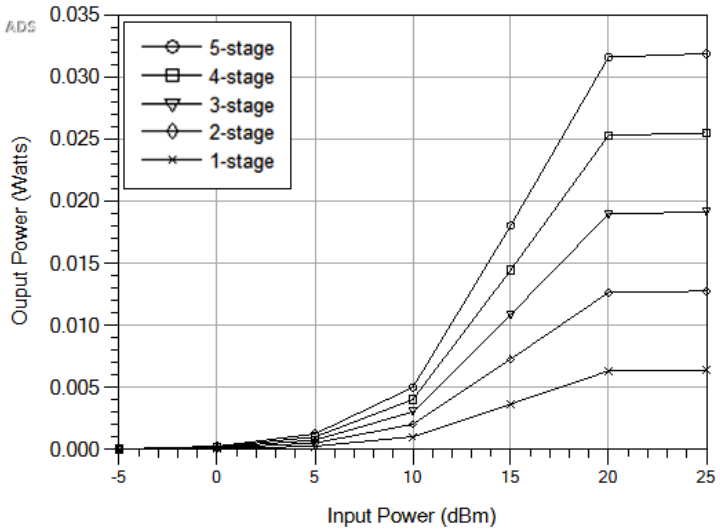

Figure 14: Effect of rectifier stages on output power at 1800 MHz.

Another important result which can be inferred from the Figure 13 and Figure 14 is the increasing trend of output power with increase in input RF power, and after

certain input RF power the output power reaches its saturation level. It can be noticed that, for each stage the output power reaches it saturation level at 20 dBm input received power. This is due to the fact that same load impedance has been used for each stage voltage rectifier i.e. 10 kΩ. If load value is varied then corresponding output power stabilizes at different input RF power e.g., if load impedance decreases the stabilizing RF power would increase and vice verse; since load impedance has inverse relation with power for a fixed voltage.

4.2.2 Overall Efficiency of The System

At the output of the first stage, the conversion efficiency of the system is usually not high, therefore the number of rectifier stages are increased to obtain higher efficiency. The overall efficiency (η) of the energy harvesting system is defined as the ratio of DC power at the output to the input received power on the receiving antenna. The graph that measures the efficiency of the system against the input received power is called *efficiency curve*. The overall efficiency of the system is defined in [35] as:

$$\eta(\%) = \frac{OutputDCPower}{InputReceivedPower} \times 100 \tag{7}$$

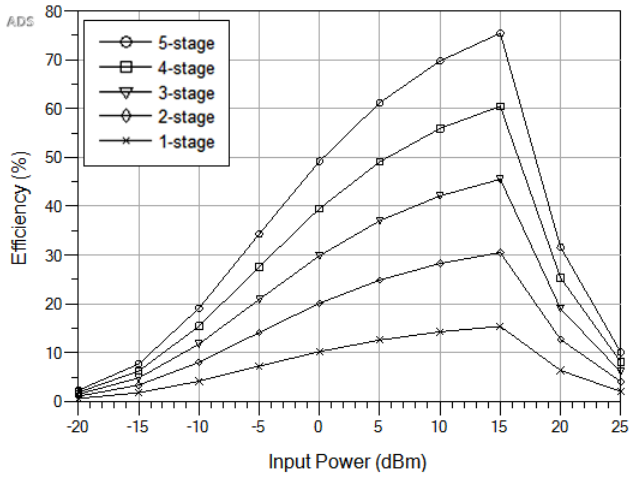

Figure 15: Effect of rectifier stages on efficiency of system at 900 MHz.

The effect of rectifier stages on the efficiency of the system can be seen from Figure 15 and Figure 16. The designed system is optimized in terms of matching network, rectifier stages and load impedance to provide maximum efficiency at both the frequencies. It can also be noticed that, for an input received power of 15 dBm and

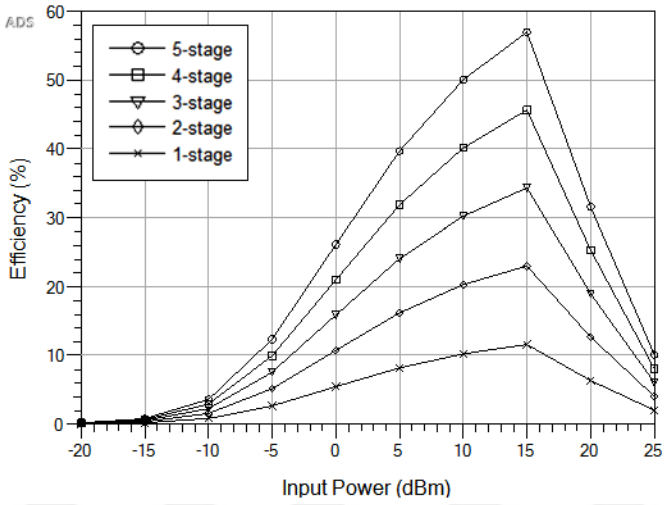

Figure 16: Effect of rectifier stages on efficiency of system at 1800 MHz.

across 10 KΩ load impedance, the highest achievable efficiencies at 900 MHz and 1800 MHz frequencies are almost 75% and 57% respectively. This shows that, efficiency of the system at higher frequency is less than the efficiency at lower frequency. Moreover, it can be seen, that after 15 dBm efficiency of the designed system decreases; because the increase in corresponding output DC power is relatively less as compared to the increase in input RF power respectively.

4.2.3 Efficiency With Respect to Different Load Impedance Levels

The load impedance should be carefully chosen for a particular energy harvesting system because it has a great impact on the performance and efficiency of the system. The effect of load impedance on the efficiency of the system is demonstrated in Figure 17 and Figure 18. ADS parameter sweep for an input received power of -20 dBm to 25 dBm and for load impedance of 10 kΩ - 160 kΩ has been used. With these

parameters the simulations are performed at both frequencies. The results show that among the tested loads, 10 kΩ load provides the highest efficiency of 75% and 57% at 900 MHz and 1800 MHz respectively. Thus, we can say that designed circuit is optimized to provide highest efficiency at 10 kΩ load under defined conditions and operating frequencies. However, when received power is lower i.e. from -20 dBm to

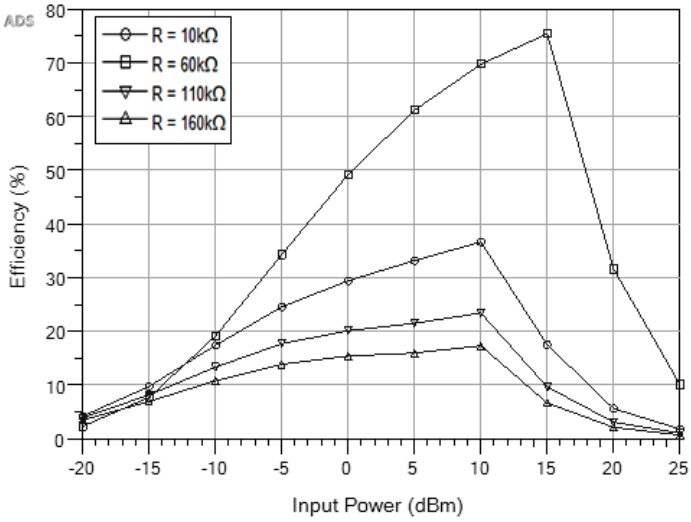

Figure 17: Efficiency of the system at different load impedance and 900 MHz.

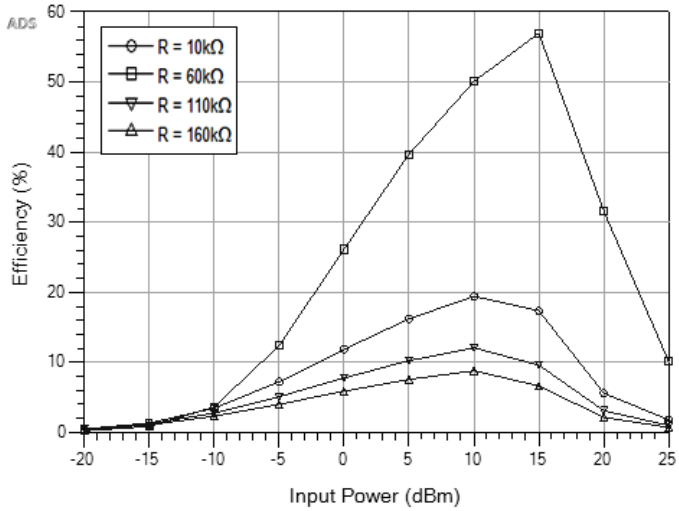

Figure 18: Efficiency of the system at different load impedance and 1800 MHz.

-12 dBm, then 60 kΩ load provides the better efficiency which can be noticed from

Figure 17. Therefore, the load impedance should be selected carefully according to the received input power and highest achievable efficiency.

4.2.4 Effect of Time at Different Distances From Transmitting Antenna

Another important parameter that effects the rate of energy harvested is the distance between the transmitting and receiving antenna. To visualize this effect receiving antenna is placed at different distances from the transmitting antenna. Simulations

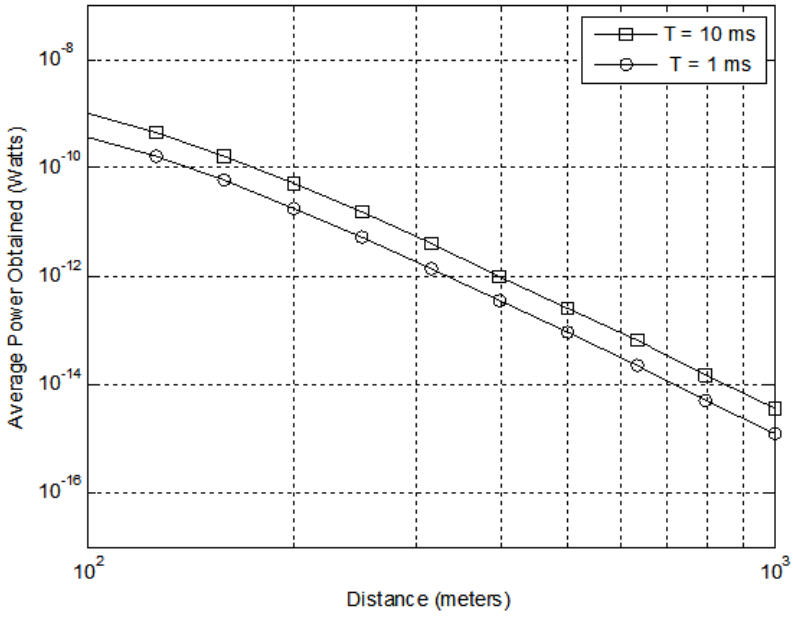

Figure 19: Average power harvested versus distance for different time instances.

are repeated for an urban environment with a parameter sweep on distance i.e. logarithmically equally spaced points between decades 10^2 meters and 10^3 meters. For transmitting frequency of 900 MHz and a fixed load impedance of 10 kΩ; the corresponding results are plotted. Figure 19 shows the graph between harvested power versus distance at a fixed source power of 100 W. It can be noticed that, average harvested power decreases with increase in distance between the transmitting and receiving antennas. In other words, if the energy harvesting device is placed closer to the RF source, then more amount of power can be harvested. Moreover, energy

harvesting rate per 1 ms is less as compared to the energy harvesting rate per 10 ms respectively. In simulation, out of considered harvesting rate (per 1 ms and per 10 ms) the power harvested for 10 ms is greater as energy stored on capacitor increases exponentially with time.

4.2.5 Effect of Transmission Power at a Fixed Time Instance

The energy harvesting rate (joules/sec) is greatly affected by the source power (P_s) of base station as shown in Figure 20. The cellular RF signal source provided by ADS design library is used to include the effect of transmitting power. The transmitting

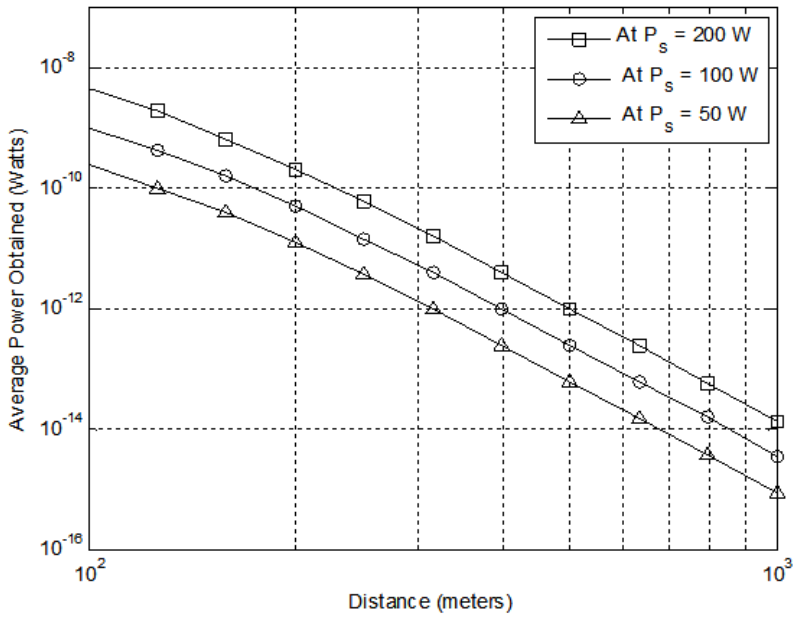

Figure 20: Effect of different source power on the harvested power.

antenna model used in mobile communication service at the base stations, is utilized for the transmission of RF signal via wireless channel. Moreover, the realistic power values are considered for the transmitting source and parameter sweep is used from 50 W to 200 W and a range of logarithmically spaced distance values from 10^2 meters and 10^3 meters has been used. The overall effect of source power on total harvested power at different values of distance and at a time instant of 5 ms has been plotted

as shown in Figure 20. It can be seen that, energy harvesting rate increases linearly with the increase in source power i.e. harvested power becomes twice if the source power is doubled.

4.2.6 Average Harvested Power Under Different Shadowing Conditions

To demonstrate the effect of signal attenuation or fading due to the obstacles in certain geographical area, different shadowing conditions have been considered in the simulations. Different terrain conditions effect the transmitted signal differently; therefore, environmental conditions should be taken into account, as it has significant effect on the energy harvesting rate. To observe the effect of shadowing, geographical conditions are varied from urban to hilly and rural. It is shown in Figure 21 that average harvested power in rural area is more than hilly terrain and urban environment, respectively. The reason behind this, is the difference in number of obstacles;

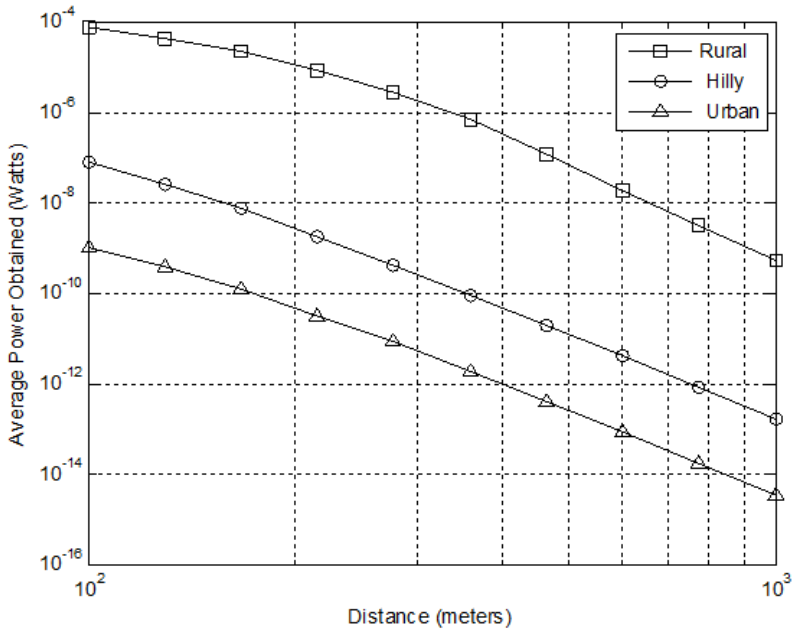

Figure 21: Average power harvested for different environmental conditions.

for example, in urban area there are more hindrances for the signal as compared to rural area. Therefore, the received signal is less attenuated in rural area and power

obtained in this case is relatively high as shown in Figure 21. Moreover, the simulated results are plotted on log-scale to better visualize the difference between energy harvesting rate under different shadowing conditions.

4.2.7 Effect of Base Station Antenna Height

The antenna height of base station is another main consideration, which effects the amount of RF signals received at a fixed distance from transmitter. If the base station antenna height is increased, pathloss decreases and when antenna height decreases, pathloss increases. Therefore, it means by increasing the antenna height, the amount of received RF signals also increases. The effect of base station antenna height on the total average power can be seen in Figure 22. In simulation environment, the base

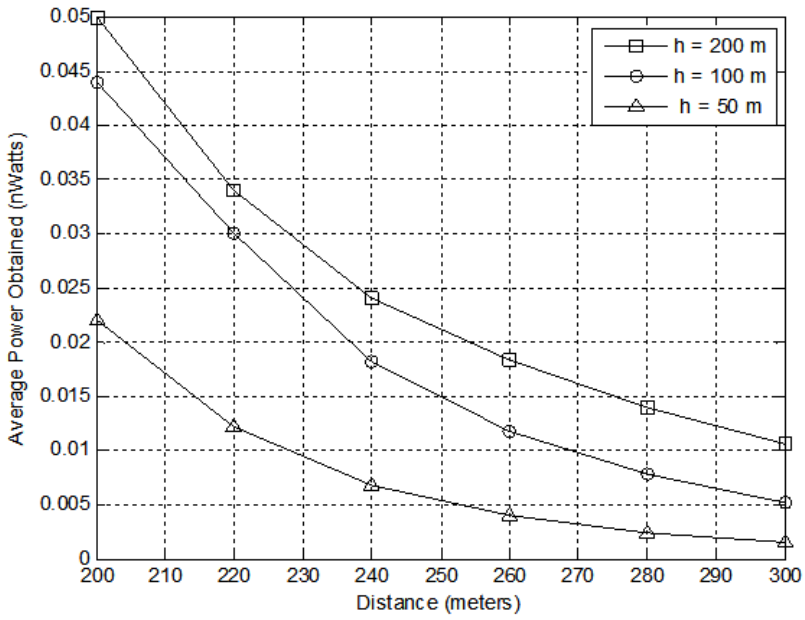

Figure 22: Average power versus distance at different base station antenna heights.

station antenna model has been used in integration with RF cellular signal source. The realistic height of transmitter has been considered by varying from 50 meters to 200 meters for a fixed source power of 100 W. The distance between transmitter and receiver has been varied from 200 meters to 300 meters, then ultimately their

effect on average power has been plotted and analyzed. It can be clearly seen, that with increase in base station height obtained average power increases, e.g., at a constant distance of 220 meters from transmitter, the corresponding harvested power at antenna height of 200 meters is more than the average power obtained at antenna height of 100 meters respectively.

CHAPTER V

ENERGY CONSUMPTION OF OPENMOTE HARDWARE

This chapter focuses on the application of RF energy harvesting in Wireless Sensor Networks (WSNs) and Internet of Things (IoT). A typical wireless sensor network consist of a collection of small autonomous devices, referred as nodes/sensors which collects the data such as temperature/humidity, light, pressure etc., from surrounding environment or certain geographical area and pass the sensed data to the main location or master node. In addition, every device in a WSN consists of a radio transceiver for wireless communication and a data processing unit known as microcontroller [36]. The block diagram of a typical sensor node is shown in Figure 23.

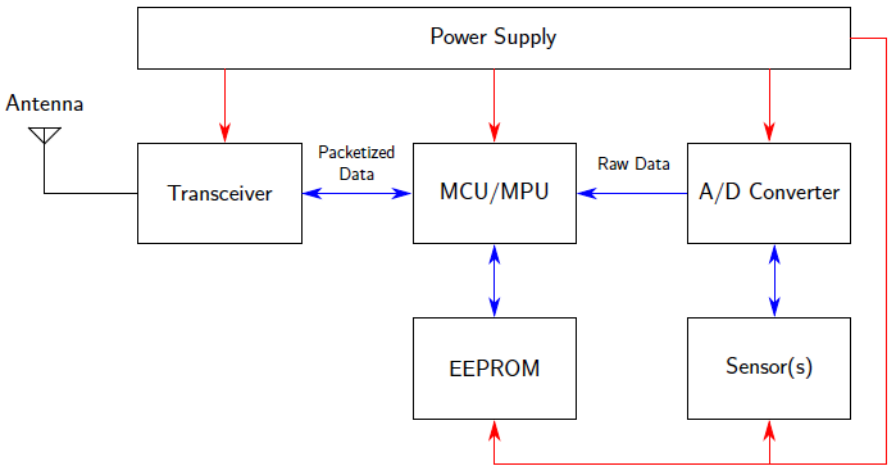

Figure 23: Block diagram of a typical sensor node [36].

Since sensing, processing and transmission/reception of data requires uninterrupted power supply to the device; therefore, the one way to supply power to the device can be done through battery. However, sometimes wireless networks are deployed at hard-to-reach places such as remote rural areas, within concrete structures,

and within human body. Therefore, in such a situation the physical replacement and maintenance of a battery is not an easy task. In the recent years, RF energy harvesting has become one of the potential solution for energizing such low power devices. RF signals are abundantly available in the atmosphere; which if harvested, allows the ubiquitous operation of the wireless network and ultimately eliminates the need of replacing batteries.

The goal of this chapter is to calculate and report the results of power consumption for one of the latest generation of Berkeley motes under different states (e.g., sensing, transmission and reception). In this regard, the OpenMote hardware system and the related interfaces have been discussed in the first section. The second section includes the operating system, which is needed for programming and code development. Finally, the experiments are performed to determine the energy consumption rate of the OpenMote-CC2538.

5.1 The OpenMote Hardware System

This section introduces the OpenMote hardware system, the accessories and the interfaces related to the system. In the presented work, OpenMote Bronze Kit has been used, which includes two OpenMote-CC2538 (the heart of the hardware system), the OpenBase board and the OpenBattery. The OpenMote Technologies provides the powerful hardware tools in order to implement and visualize WSNs and IoT applications [19]. Moreover, the hardware has simpler and attractive design as the calculation/communication board is separated from the interface board. The details of each interface of the OpenMote kit is further elaborated in the next subsections.

5.1.1 OpenMote-CC2538

The OpenMote-CC2538 is the fundamental part of the OpenMote hardware technology, as shown in Figure 24. It can be connected to the other interfaces of OpenMote

hardware kit such as OpenBase and OpenBattery. When connected to the OpenBattery, it integrates with the various sensors and independently act as a node. If it is connected with the OpenBase, it can be programmed for firmware development.

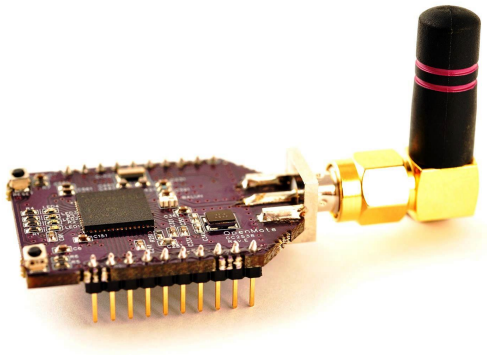

Figure 24: An OpenMote-CC2538 [19].

The brain of the OpenMote-CC2538 is the Texas Instrument (TI) CC2538 System-on-Chip (SoC) powerful wireless micro-controller; which can be used for many wireless applications such as smart grids, WSNs and IoT. The ARM 32-bit Cortex microcontroller has a clock speed up-to 32 MHz, in-system programmable flash up-to 512 KB and up-to 32 KB of RAM memory [37]. The radio transceiver operates at 2.4 GHz Zigbee IEEE 802.15.4 standard, with an excellent receiver sensitivity of -97 dBm and a programmable output power of +7 dBm. Moreover, the OpenMote has low power consumption; when the receiving mode is active the mote consumes 20 mA of current at 0 dBm and during the transmission mode the current consumption is around 24 mA. Figure 25 shows the functional block diagram of CC2538 including the details of radio transceiver, serial interfaces and other peripherals.

The TPS62730 is a Texas Instrument high frequency step down DC/DC converter with two operating modes: the ultra low-power bypass mode and regulated mode. In the regulated mode, the input voltage is reduced from typically 3 V to 2.1 V during

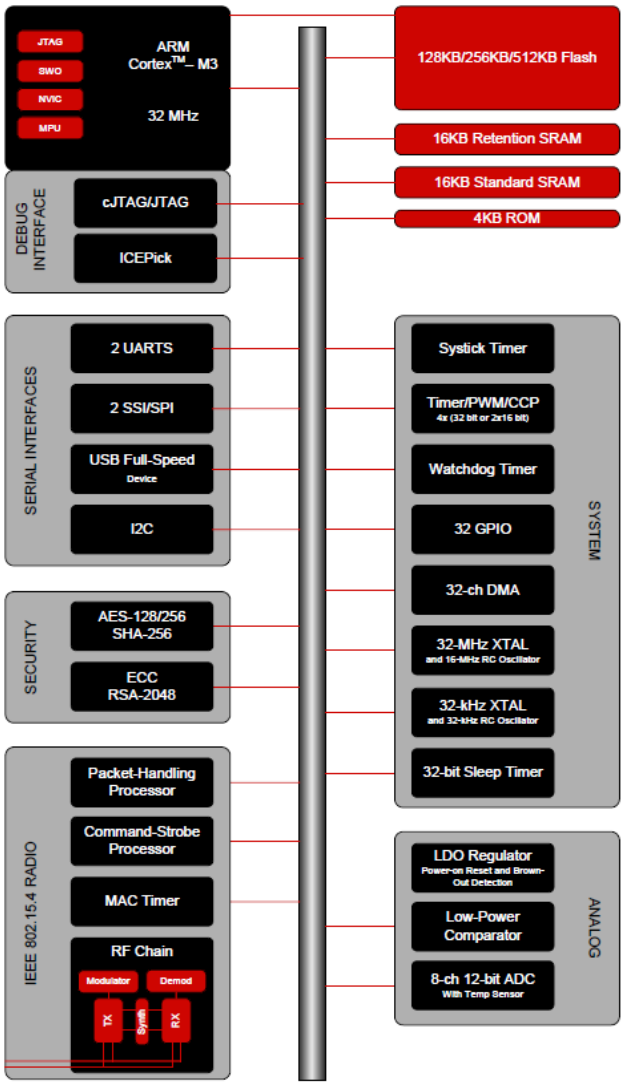

Figure 25: CC2538 functional block diagram [37].

transmission and reception by an highly efficient voltage converter. In ultra low-power bypass mode, the current consumption is reduced further to support the low power modes such as sleep mode. The advantage of this approach is that, the efficiency of the system can be improved under both high-load (transmitting or receiving) and low-load conditions (sleep mode) [38].

Moreover, the device also featured a ABM8G 32 MHz crystal for the radio and CC2538 microcontroller. The crystal is off when there is no transmission/reception

and the radio is in sleep mode. ABS07 a second crystal of 32.768 kHz is used to clock the microcontroller's Real Time Clock (RTC). The use of second crystal helps attaining attractive time synchronization and allows the OpenMote to keep record of time even in the deep-sleep state.

Last but not the least, the OpenMote-CC2538 includes 4 LEDS of different colors for visualizing the debugging process and 2 push buttons; one for resetting the mote and the other button for activating the microcontroller from the sleep mode. In addition, an SMA connector is also attached with the board for connecting an external antenna which can be used during transmission and reception. The design and shape of output pins is compatible to any other device with similar XBee interface (e.g., WaspMote); thus, it adds to the usage versatility of OpenMote [19].

5.1.2 OpenBase

The OpenMote hardware also includes an interface board known as OpenBase (shown in Figure 26), which provides all the necessary interfaces that helps in prototyping and firmware development for the OpenMote-CC2538. The board is featured with current sense pins, that can be used to measure the current drawn by OpenMote during different operations and conditions.

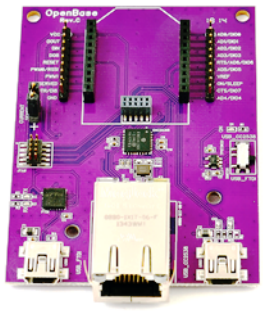

Figure 26: The OpenBase interface board [19].

It is equipped with two 10-pin XBee headers for connecting the OpenMote and a 10-pin JTAG connector for debugging the OpenMote [38]. The multipurpose board

shown in Figure 26 serves different functions. The JTAG interface provides real time debugging capabilities during program development such as, breakpoints support and inspecting variables through a debugging probe. The commonly used debugging probe is Segger J-Link EDU, which can be connected to the board through 20 - 10 pin ARM JTAG adapter. Moreover, Openbase provides a USB connector that allows the communication of board with computer and is also used to program and debug the OpenMote-CC2538. It enables the communication through 10/100 Mbps ethernet interface which directly connects the OpenMote-CC2538 to the Internet without using the computer [38]. This ethernet connectivity is based upon the ENC28J60 microchip (a stand-alone ethernet controller) and a standard physical network interface (RJ-45 connector) is used for connecting the LAN cable.

5.1.3 OpenBattery

The OpenBattery (see Figure 27) act as an interface board for the OpenMote-CC2538. It provides power to the OpenMote and is equipped with sensors. The 2 × AAA battery socket is present just beneath the OpenBattery, which provides energy to the device in order to operate independently as a node [19].

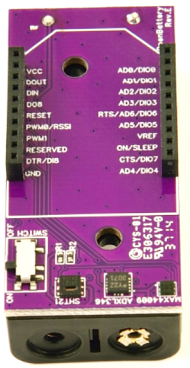

Figure 27: The OpenBattery [19].

The device has 20-pin XBee socket that allows OpenMote-CC2538 to be easily plugged in and plugged out without soldering. It also includes three digital sensors:

an ambient light sensor (MAX44009), a humidity/temperature sensor (SHT21) and an ultra low power 3-axis acceleration sensor (ADXL346). These sensors start sensing the data, immediately after the switch is powered on. Each sensor is integrated with the OpenMote via I2C bus having two lines, Serial Data Line (SDA) and Serial Clock Line (SCL).

5.2 OpenMote Software System

The OpenMote hardware and the related interfaces can be enabled by the OpenMote software system. Some specifically designed open source software for IoT applications such as, Contiki and OpenWSN are fully supported by OpenMote-CC2538. In our work, we have used Contiki Operating System (OS) for software development and its details are discussed in the next section.

5.2.1 Contiki Operating System

Contiki is a highly powerful open source operating system specifically designed for WSNs and IoT, which connects the extremely low-power microcontrollers to the Internet. It is highly memory efficient and provides fast and easy development of complex wireless system. It runs on variety of low-power devices and fully supports the IPV4 and IPV6 standards including various low-power wireless protocols, such as IPV6 over Low-Power Wireless Personal Area Network (6lowpan), Routing Protocol (RPL) and Constrained Application Protocol (CoAP) etc. In addition, it provides full IP networking with standard IP protocols such as TCP, UDP and HTTP. The first layer of the contiki netstack is the radio/physical layer which is usually a low-power hardware; CC2538 radio transceiver in our case. In the MAC layer, the outgoing queued packets are transmitted through the Radio Duty Cycling (RDC) layer, which in turn transmit through the radio link layer (IEEE 802.15.4) [39]. The sender receives an acknowledgement (ACK) from the receiver in case of successful transmission, otherwise MAC layer will continue to retransmit the packet until a link layer ACK is received.

5.3 Measurement of Power Consumption in OpenMote

This section presents the energy consumption rate of the OpenMote-CC2538 in different states. The main components which consume the power during certain operation or task, is the microcontroller and the radio transceiver. The required power consumed during different operations, and for a certain time t, can be calculated using the following equation:

$$P_{consumed} = \frac{1}{T} \int_0^t V I_c dt \tag{8}$$

Where, V is the supplied/operational voltage of the OpenMote which is usually in the range of (2 V - 3.6 V), I_c is the amount of current drawn/consumed during different operations and T is the total time period. The power consumed during data sensing, transmission and reception, at different transmitting power and the effect of packet size has been calculated by performing different experiments and finally the results have been recorded.

5.3.1 Experimental Setup

For our experiments, the developed program is flashed on the OpenMote-CC2538 via USB interface. For measuring the current, Keysight digital multimeter 34411A has been used which is much more powerful and has enhanced performance as compared to ordinary multimeter. For this purpose, the current sense pins on the OpenBase are connected to the corresponding probes of the digital multimeter. Since there is high variation in the measured current values with respect to time, therefore to visualize the consumed current more accurately the digital multimeter is connected to the computer via GPIB interface. Keysight BenchVue software is used to record measurements from digital multimeter on a computer. Moreover, this software also provides graphical view of the varying data w.r.t time, which helps to better understand the behaviour of recorded measurements. The experimental setup for measuring energy consumption rate is shown in Figure 28.

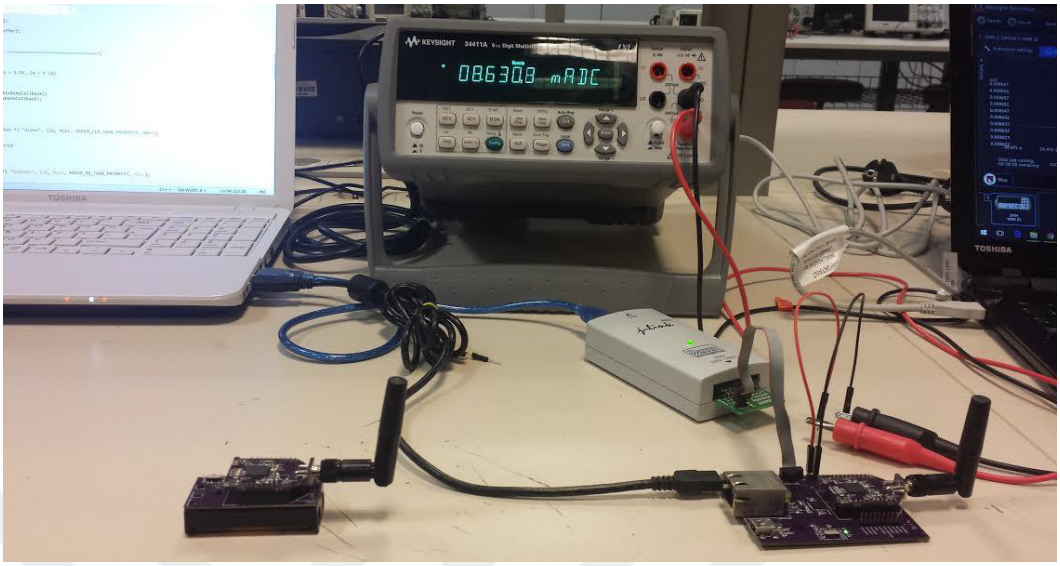

Figure 28: The experimental setup for measurement of power consumption.

5.3.2 Average Power Demand of Sensing Operation

The mote is programmed to perform single and multiple sensing per second and the corresponding current is measured for each sensor. The maximum of 6 sensing operations per second have been considered and Figure 29 shows the current consumption during temperature sensing.

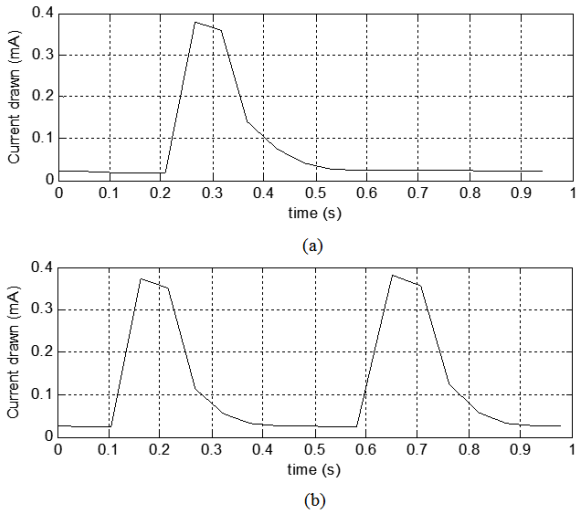

Figure 29: Current consumption of OpenMote. (a) 1-sensing/sec. (b) 2-sensing/sec.

It can be seen, that the current drawn by the OpenMote during sensing is almost 0.37 mA, which is in accordance with the data sheet of OpenMote-CC2538. Once the current consumption is known, the energy consumption rate during sensing can be calculated using equation (8) by applying the numerical integration over the time interval. Figure 30 shows the trend of number of sensing versus rate of energy consumption. It can be noticed that, when the mote is programmed to take more readings per seconds, the energy consumed per second is higher. Therefore, the graph shows the linear increasing trend with increase in the number of sensing operations for all the sensors.

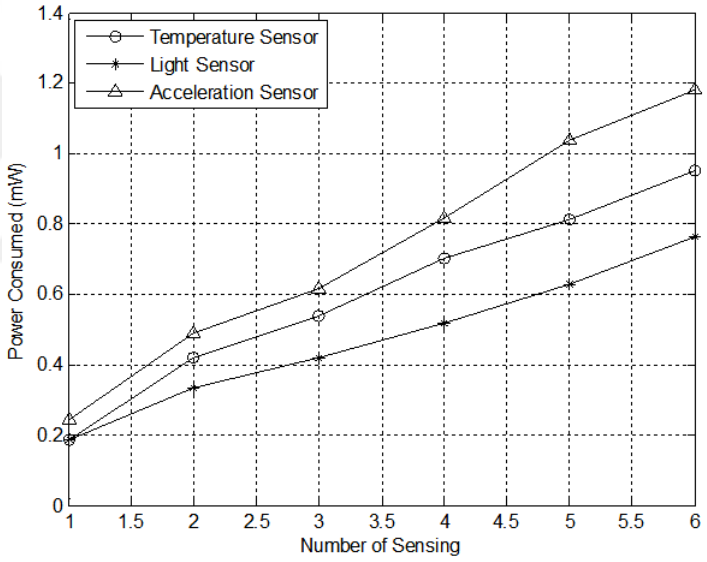

Figure 30: Power consumption of various sensors in OpenMote.

5.3.3 Power Consumption During Data Transmission

For measuring the current consumption during data transmission, the OpenMote-CC2538 is set to the transmission mode and data packets are transmitted at a certain power level. Figure 31 shows the current consumption of OpenMote in a transmission mode and with two different transmitted powers, i.e. 0 dBm and 7 dBm. It can be seen that, the current consumption is higher at high transmission power as compared

to the current consumption at low transmission power. In other words, for a fixed time interval and a packet size, the current consumption is almost 34 mA and 24 mA at the transmission power of 7 dBm and 0 dBm respectively.

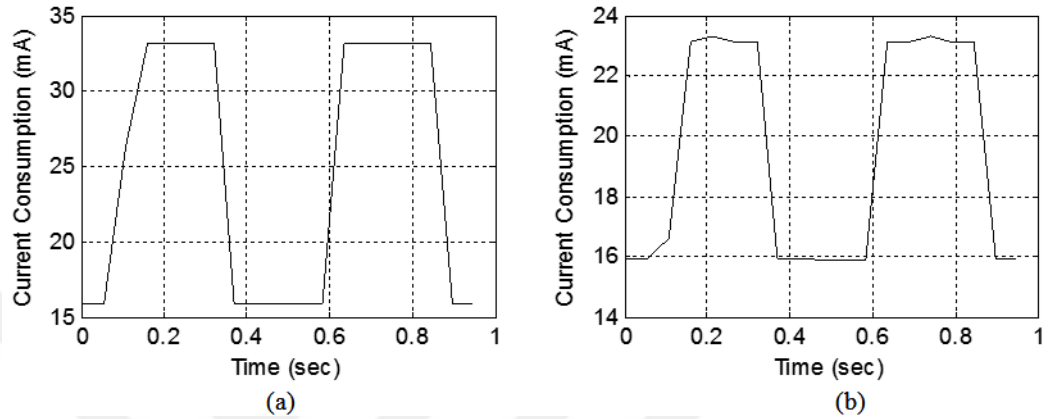

Figure 31: Current consumption at transmitting power of (a) 7 dBm. (b) 0 dBm.

OpenMote IEEE 802.15.4 zigbee radio transceiver has maximum packet size of 128 bytes. Therefore, the packet size is varied from 26 - 125 bytes to calculate the consumed average power. Figure 32 shows the trend of power consumption demand

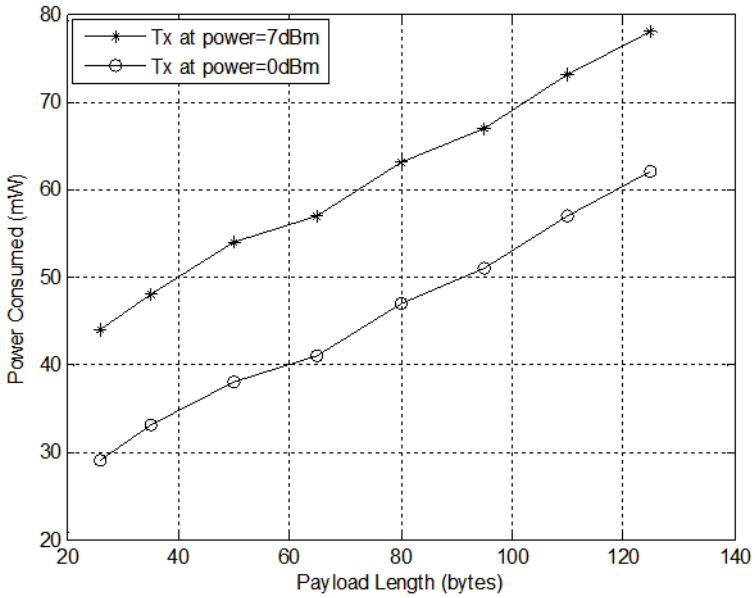

Figure 32: Power consumption during transmission at different transmitting powers.

versus range of data packet lengths at different transmission power (e.g., 0 dBm and 7 dBm). It can be noticed that, the power consumption increases linearly by increasing the packet size of transmitted data. Furthermore, the energy consumption rate at two transmitted power levels are compared and it reveals that by increasing the power of transmitted signal, the rate of energy consumed by transmitter mote increases. Therefore, the power consumption of transmitting mote at 7 dBm is higher than the power consumed at 0 dBm.

5.3.4 Power Consumption During Reception

Figure 33 shows the current consumption of the OpenMote-CC2538 at different distances from the transmitting node. It can be seen that, as the distance between the

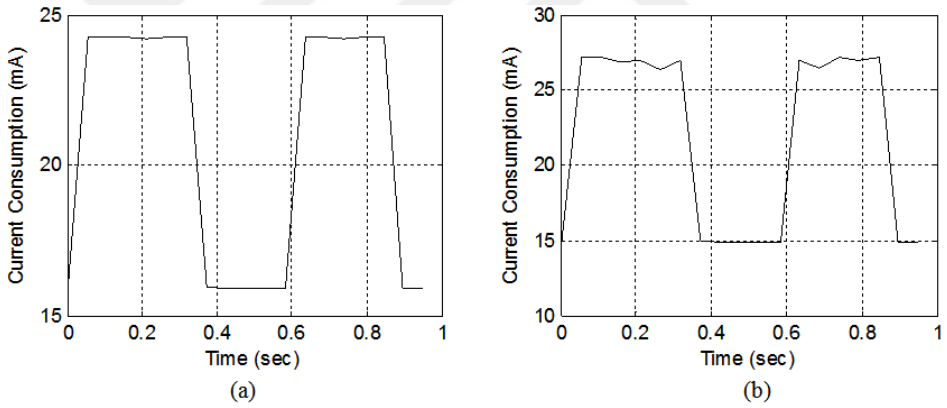

Figure 33: Current consumption during reception at distance of. (a) 5 m. (b) 10 m.

transmitting and the receiving device increases, the signal received at the receiving end will be of low strength; which ultimately results in more current consumption. It can be inferred that, for a fixed packet size and a time duration, the current consumption is approximately 26 mA and 24.5 mA at a distance of 10 m and 5 m from the transmitting node, respectively.

Figure 34 shows the energy consumption rate during the reception at different distances from the transmitter mote. The mote is programmed to transmit a packet, which is received by the receiving mote placed at different distances (i.e. from 1 meter

to 10 meters). For 7 dBm transmitting power and the different packet length of data, the corresponding rate of energy consumed is calculated by measuring the current drawn. The effect of distance on the rate of energy consumption can be noted from this figure, when the distance between the transmitting and the receiving mote is varied from 1 m to 10 m, the energy required to retrieve the signal is also increased because signal strength decreases with increase in distance.

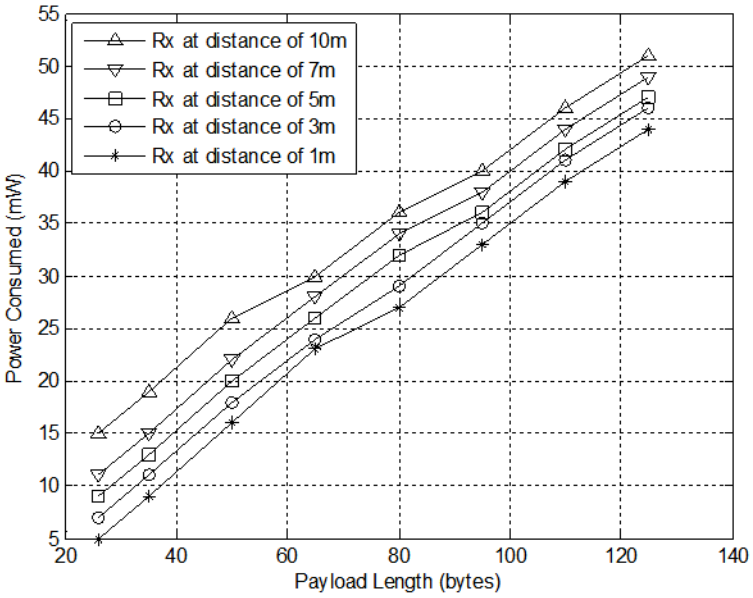

Figure 34: Power consumption during reception at input power of 7 dBm.

Figure 35 shows the similar result as in Figure 34, except the transmitting power which is set to be 0 dBm. When the packet is transmitted at low transmitting power (0 dBm), the power consumed during reception is more as compared to the packet transmitted at high transmitting power (7 dBm). In other words, the power consumed during reception is inversely proportional to the transmitting power, because of the fact that mote consumes more power in receiving a packet with less RF power. For example, at a fixed data size of 126 bytes and a distance of 10 meters from transmitter, power consumed against transmitting power of 0 dBm and 7 dBm is 59 mW and 51 mW respectively.

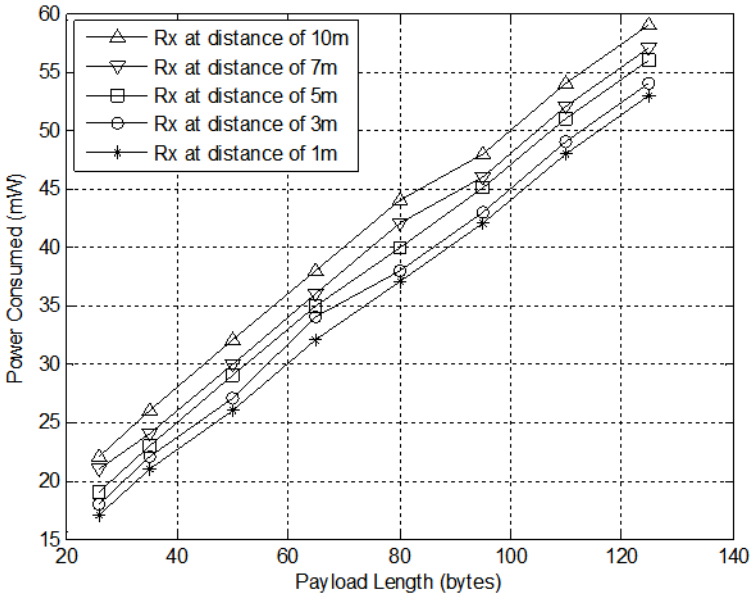

Figure 35: Power consumption during reception at input power of 0 dBm.

5.3.5 Active and Sleep Mode Current Consumption

The OpenMote's CPU (microcontroller) is programmed to run at 32 MHz and 16 MHz crystal. When the CPU runs at 32 MHz, the OpenMote-CC2538 consumes 13 - 14 mA, whereas for 16 MHz clock configuration, current consumption decreases to 7 mA. It is known that when CPU performs tasks requiring 16 MHz, will consume

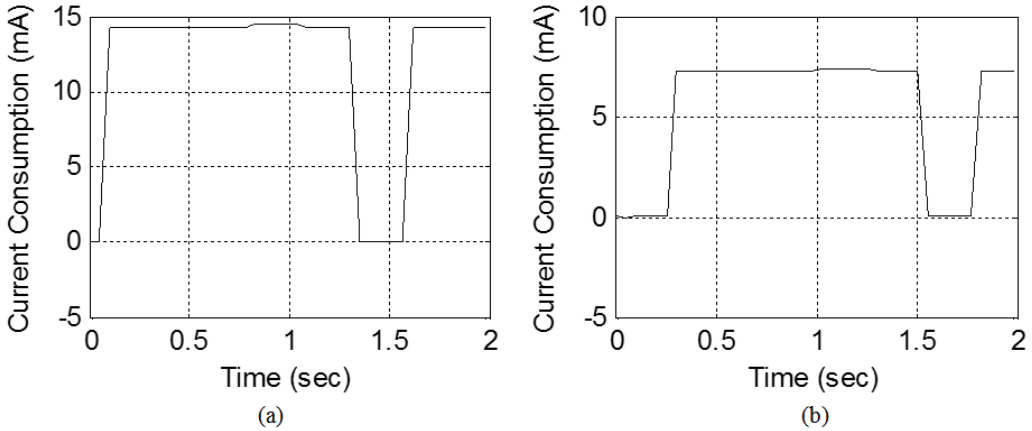

Figure 36: Current consumption at clock speeds of (a) 32 MHz. (b) 16 MHz.

less current, while 32 MHz operations draws more current as shown in Figure 36 (a, b) respectively. OpenMote-CC2538 is programmed such that, CPU switches from running mode to sleep mode/idle mode after 750 ms. CPU remains in sleep mode for 250 ms and current consumption in this state has been decreased to 1.4 μA as shown in Figure 36 (well agreement with the data sheet value).

5.4 Discussion and Analysis

After the power consumption demand of OpenMote has been estimated, the next main task is to compare the power harvested from our designed system and power consumption results. In the previous chapter, RF energy harvesting circuit has been

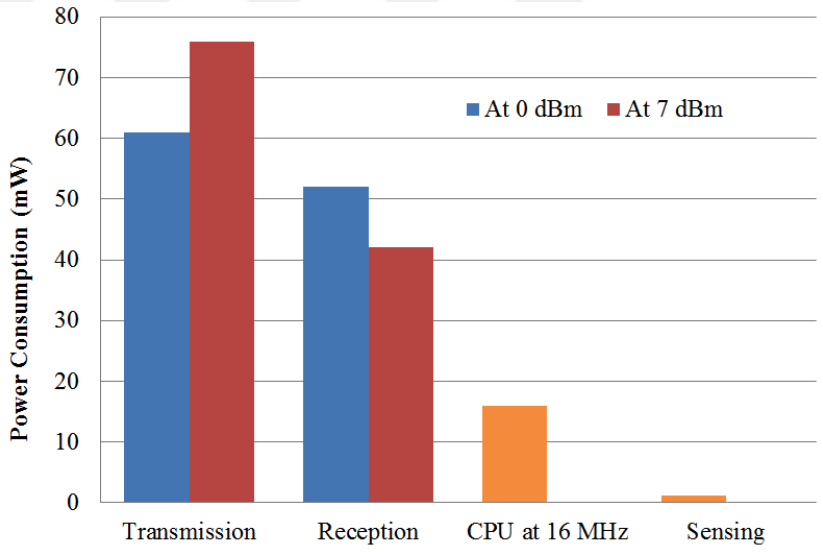

Figure 37: Power consumption of OpenMote during various operations.

designed and analyzed under different parameters which effects the total output power of the system. Moreover, it has been evaluated that system is optimized to provide highest efficiency at 10 kΩ, whereas, OpenMote also translates as 10 kΩ load during sensing because it draws 0.37 mA current in this mode, provided that operating voltage is around 3.3 V. Our power consumption analysis reveals that, OpenMote

requires 0.25 mW power to perform sensing as shown in Figure 37; whereas, our designed energy harvesting system can provide comparable power for sensing operation of OpenMote.

Since our designed energy harvesting system has been made more practical by including channel impairments and pathloss; therefore, such system usually may not be able to completely energize all the operations of OpenMote, such as transmission and reception. However, if multiple receiving antennas e.g., antenna arrays are incorporated, then input RF power can be increased; which ultimately enhances the output harvested power. In addition to this, if designed system simultaneously harvests from dual cellular frequencies i.e. both frequencies are utilized, it will ultimately increase the total amount of power obtained. For example, if 0 dBm of RF power is incident on receiving antenna of our designed system, then proposed system can provide 0.5 mW power which is sufficient to energize the OpenMote to perform one sensing operation i.e. 0.25 mW. Moreover, with increase in input RF power more energy can be harvested, which in turn may energize OpenMote for performing multiple tasks.

CHAPTER VI

CONCLUSION AND FUTURE WORKS

The presented thesis is based upon two folds aspects; firstly, dual band RF energy harvesting system for cellular base station has been designed and analyzed in detail. The receiving antenna, matching network and 5-stage voltage rectifier has been optimized to make the designed system efficient equally on both frequencies. Our system provides almost 75% and 57% efficiencies at 900 MHz and 1800 MHz respectively. Moreover, wireless channel and transmitting source has been introduced in the simulation setup, to investigate their effect on harvested power under different geographic conditions.

Second part of the presented work focuses on the application of RF energy harvesting in WSNs. For uninterrupted operation of such sensors, battery source needs to be physically recharged or replaced, which is not an efficient approach. Another potential solution to energize these low power wireless devices is enabling the nodes to harvest RF energy directly from environment. In this regard, it is important to estimate the power consumption demand of such low-power wireless network. Therefore, our research aims to investigate the overall power consumption for one of the latest generation of Berkeley motes under different states (e.g., sensing, transmission and reception). For this purpose, OpenMote hardware kits have been used, which includes actual wireless sensor node that can perform various operations under different conditions. It can be inferred from the experimental data, that OpenMote consumes almost 61 mW of power during the transmission of 120 bytes payload. Similarly, at transmission power of 0 dBm, and at a distance of 1 meter, the mote requires 52 mW of power for data reception. Whereas, sensing operation has overall less power

demand, i.e. 1.2 mW power is required for 6-sensing operations.

Since the practical implementation of RF energy harvesting needs to consider many important factors, such as parasitic losses and PCB fabrication losses. The harvested energy in a practical scenario is different than the simulation setup. Therefore, these consideration should be taken into account to implement the energy harvesting system with minimum losses. Moreover, in order to have enhanced performance and cost efficient design, the circuit needs to be implemented as System on Chip (SoC) as it experiences less parasitic losses, and it will be considered in our future work. Moreover, practical integration of energy harvesting circuit with OpenMote wireless sensor network is also one of the important consideration for our future work. Consequently, instead of relying on the battery cells the motes will utilize the energy harvested from the designed harvesting circuit.

Bibliography

[1] B. Insider, *The Internet Of Things Will Be Bigger Than The Smartphone, Tablet, And PC Markets Combined*, Oct. 2014. Available at http://www.businessinsider.com/the-internet-of-things-market-growth-2014-9.

[2] X. Lu, P. Wang, D. Niyato, D. Kim, and Z. Han, "Wireless networks with RF energy harvesting: A contemporary survey," *IEEE Communication Survey and Tutorials*, vol. 17, pp. 757–789, May 2015.

[3] U. Sengupta, *Energy Harvesting*, Nov. 2013. available at www.batterypoweronline.com/main/blogs/energy-harvesting-is-there-no-free-lunch/.

[4] A. Didioui, "Energy-aware transceiver for energy harvesting wireless sensor networks," Master's thesis, Universite de Rennes, France, 2014.

[5] T. Soyata, L. Copeland, and W. Heinzelman, "RF energy harvesting for embedded systems: A survey of trade offs and methodology," *IEEE Circuits and Systems Magazine*, vol. 16, pp. 22–57, Feb. 2016.

[6] L. T. Beng, L. N. Meng, P. B. Kiat, and T. kyaw, "Pervasive RF energy harvesting system (GSM 900 and GSM 1800)," *IEEE Conference on Technologies for Sustainability (SusTech)*, pp. 273–276, July 2014.

[7] M. S. Alam and S. Moury, "Multiple-band antenna coupled rectifier circuit for ambient RF energy harvesting for WSN," *International Conference on Informatics, Electronics and Vision (ICIEV)*, pp. 1–4, May 2014.

[8] S. Ghosh and A. Chakrabarty, "Dual band circularly polarized monopole antenna design for RF energy harvesting," *IETE Journal of Research*, vol. 62, pp. 9–16, Aug. 2015.

[9] G.1ndumathi and K.Karthika, "Rectenna design for RF energy harvesting in wireless sensor networks," *IEEE International Conference on Electrical, Computer and Communication Technologies (ICECCT)*, pp. 1–4, Mar. 2015.

[10] M. Arrawaita, M. S. Baghini, and G. kumar, "RF energy harvesting systems from cell towers in 900 MHz band," *National Conference On Communications (NCC)*, pp. 1–5, Jan. 2011.

[11] N. M. Din, C. K. Chakrabarty, A. B. Ismail, K. K. A. Devi, and W. Y. Chen, "Design of RF energy harvesting system for energizing low power devices," *Progress in Electromagnetics Research (PIER)*, vol. 132, Sept. 2012.

[12] F. Alneyadi, M. Alkaabi, S. Alketbi, S. Hajraf, and R. Ramzan, "2.4 GHz WLAN RF energy harvester for passive indoor sensor nodes," *IEEE International Conference on Semiconductors Electronics (ICSE)*, pp. 471–474, Aug. 2014.

[13] J. H. Kim, J. Bito, and M. Tentzeris, "Design optimization of an energy harvesting RF-DC conversion circuit operating at 2.45 GHz," *IEEE International Symposium on antennas and Propagation and USNC/URSI National Radio Science Meeting*, pp. 1280–1281, July 2015.

[14] A. Sample and J. R. Smith, "Experimental results with two wireless power transfer systems," *IEEE Radio Wireless Symposium (RWS)*, pp. 16–18, Jan. 2009.

[15] T. Ungan and L. M. Reindl, "Harvesting low ambient RF sources for autonomous measurement systems," *IEEE Instrumentation and Measurement Technology Conference (IMTC)*, pp. 62–65, May 2008.

[16] H. J. Visser and R. J. Vullers, "RF energy harvesting and transport for wireless sensor network applications: principles and requirements," *Proceedings of IEEE*, vol. 101, pp. 1410–1423, Apr. 2013.

[17] D. Pavone, A. Buonanno, M. D'Urso, and F. D. Corte, "Design considerations for radio frequency energy harvesting devices," *Progress in Electromagnetics Research (PIER)*, vol. 45, pp. 19–35, Oct. 2012.

[18] A. M. Zungeru, L.-M. Ang, S. Prabaharan, and K. P. Seng, *Radio Frequency Energy Harvesting and Management for Wireless Sensor Networks*. available on-line at arXiv:1208.4439.

[19] X. Vilajosana, P. Tuset, T. Watteyne, and K. Pister, "Openmote: Open-source prototyping platform for the industrial IoT," *7th International Conference on Ad Hoc Networks (AdHocNets)*, Sept. 2015.

[20] E. Casilari, J. M. Cano-Garcia, and G. Campos-Garrido, "Modeling of current consumption in 802.15.4/zigbee sensor motes," *Sensors*, vol. 14, pp. 5443–5458, May 2010.

[21] X. Vilajosana, Q. Wang, F. Chraim, T. Watteyne, T. Chang, and K. S. J. Pister, "A realistic energy consumption model for TSCH networks," *IEEE Sensors Journal*, vol. 14, pp. 482–489, Feb. 2014.

[22] D. W. Harrist, "Wireless battery charging system using radio frequency energy harvesting," Master's thesis, University of Pittsburgh, Pittsburg, USA, 2004.

[23] S. Shrestha, S. Noh, and D.Choi, "Comparative study of antenna designs for RF energy harvesting," *International Journal of Antennas and Propagation*, vol. 2, Jan. 2013.

[24] Z. Zakaria, N. A. Zainuddin, M. N. Husain, M. Z. A. Aziz, M. A. Mutalib, and A. R. Othman, "Current developments of RF energy harvesting system for wireless sensor networks," *International Journal on Advances in Information Sciences and Service Sciences(AISS)*, vol. 5, June 2013.

[25] O. Amjad, S. W. Munir, S. T. Imeci, and A. O. Ercan, "Ambient WLAN RF energy harvesting system with dual-band microstrip patch antenna," *5th Asia Pacific Conference on Antennas and Propagation (APCAP)*, July 2016.

[26] C. Balanis, *Antenna Theory: Analysis and Design*. Newyork, USA: John Wiley and Sons, Inc., 2nd ed., 1998.

[27] M. C. Huynh and W. Stutzman, "Ground plane effects on planar inverted-F-antenna (PIFA) performance," *IEEE Proceedings - Microwaves, Antennas and Propagations*, vol. 150, pp. 209–213, Aug. 2003.

[28] M. H. Hoang, V. H. Nguyen, T. Q. V. Hoang, and T. P. Vuong, "Co-design of dual-band GSM filtenna based on printed-IFA for energy harvesting," *10th Conference on PhD in Microelectronics and Electronics (PRIME)*, Aug. 2014.

[29] N. Firoozy and M. Shirazi, "Planar inverted-F-antenna (PIFA) design dissection for cellular communication application," *Journal of Electromagnetic Analysis and Applications*, pp. 406–411, Oct. 2011.

[30] S. W. Munir, O. Amjad, E. Zeydan, and A. O. Ercan, "Optimization and analysis of WLAN RF energy harvesting system architecture," *13th International Symposium on Wireless Communication Systems (ISWCS)*, pp. 429–433, Oct. 2016.

[31] D. J. Lopez and I. A. E. Atienzar, "Powering autonomous sensors by RF harvesting," Master's thesis, Universitat Politecnica de Catalunya, Spain, 2013.

[32] K. K. A. Devi, N. Md.Din, C. K. Chakrabarty, and S. Sadasivam, "Design of an RF - DC conversion circuit for energy harvesting," *IEEE International Conference on Electronics Design, Systems and Applications (ICEDSA), 2012*, Nov. 2012.

[33] J. Zhang and Z. Jia, "Design of voltage doubling rectifier circuit in wireless sensor networks," *IEEE International Conference on Progress in Informatics and Computing (PIC)*, Jan. 2011.

[34] P. Nintanavongsa, U. Muncuk, D. R. Lewis, and K. R. Chowdhury, "Design optimization and implementation for RF energy harvesting circuits," *IEEE Journal on Emerging and Selected Topics in Circuits and Systems*, vol. 2, pp. 24–33, Mar. 2012.

[35] J. Curty, N. Joehl, C. Dehollain, and M. Declercq, "Remotely powered addressable UHF RFID integrated system," *IEEE Journal of Solid-State Circuits*, vol. 40, pp. 2193–2202, Nov. 2005.

[36] A. D. Mauro, "On the impact of energy harvesting on wireless sensor network security," Master's thesis, Technical University of Denmark, Denmark, 2014.

[37] T. Instruments, *CC2538 Powerful Wireless Microcontroller System-On-Chip for 2.4-GHz IEEE 802.15.4, 6LoWPAN, and ZigBee Applications*, Apr. 2015. available at http://www.ti.com/lit/ds/symlink/cc2538.pdf.

[38] T. Chang, P. Tuset-Peiro, X. Vilajosana, and T. Watteyne, "OpenWSN and openMote: Demoing a complete ecosystem for the industrial internet of things," *13th Annual IEEE International Conference on Sensing, Communication, and Networking (SECON)*, June 2016.

[39] M. Ojo, D. Adami, and S. Giordano, "Performance evaluation of energy saving MAC protocols in WSN operating systems," *International Symposium on Performance Evaluation of Computer and Telecommunication Systems (SPECTS)*, July 2016.